Mathematics

https://www.aimspress.com/journal/Math

AIMS Mathematics, 10(10): 25049–25084.
DOI: 10.3934/math.20251110
Received: 13 June 2025
Revised: 06 October 2025
Accepted: 15 October 2025
Published: 31 October 2025

Research article

Dynamic analysis of a fractional-order HIV/AIDS model with generalized nonlinear incidence rate

Mi Yang[1], Da-peng Gao[1,2,3,*], Shi-qiang Feng[3] and Jin-dong Li[4]

[1] School of Mathematical Sciences, China West Normal University, Nanchong, Sichuan 637009, China

[2] Sichuan Colleges and Universities Key Laboratory of Optimization Theory and Applications, China West Normal University, Nanchong, Sichuan 637009, China

[3] Institute of Nonlinear Analysis and Applications, China West Normal University, Nanchong, Sichuan 637009, China

[4] School of Mathematical Sciences, Chengdu University of Technology, Chengdu, Sichuan 610059, China

* **Correspondence:** Email: dapenggao@cwnu.edu.cn.

Abstract: This paper investigates a fractional-order human immunodeficiency virus (HIV)/acquired immune deficiency syndrome (AIDS) model with generalized nonlinear incidence rates $f(S, I)$ and $g(S, E)$. First, the existence, uniqueness, non-negativity, and boundedness of the model solutions are proven, and the basic reproduction number R_0^α is derived. The analysis indicates that the model exhibits two equilibrium points: A disease-free equilibrium and an endemic equilibrium. The local asymptotic stability of each equilibrium point is examined using the Routh-Hurwitz criterion. Additionally, by employing Lyapunov functionals and applying LaSalle's invariance principle, the global stability of the equilibrium points is demonstrated. The main conclusion is that under appropriate conditions, if $R_0^\alpha < 1$, then the disease will eventually disappear, whereas if $R_0^\alpha > 1$, then it will persist. Finally, the model is utilized to predict and control of HIV/AIDS transmission in Mexico, thereby highlighting the role of mutural preventive measures adopted by susceptible individuals and HIV-infected individuals in reducing disease spread. Simulations are performed to confirm the theoretical validity and practical significance of the model.

Keywords: caputo fractional derivative; reproduction number; local stability; global stability
Mathematics Subject Classification: 26A33, 34A08, 37N25

1. Introduction

Since the first case of HIV infection was reported in 1981, humans have been battling it for more than 40 years [1]. In 2022, the number of people infected with human immunodeficiency virus (HIV) worldwide has exceeded 37.7 million, remains a severe threat to the global community. HIV can be transmitted through the blood, semen, cervical secretions, and breast milk. People infected with HIV lack the necessary protective awareness and active treatment, which results in an impaired immune system, and eventually develops into acquired immune deficiency syndrome (AIDS). To date, there is no specific drug or vaccine has been developed to completely eradicate HIV; however, antiretroviral therapies have played a crucial role in prolonging the life of infected people and reducing the risk of viral transmission [2]. Fortunately, from 2000 to 2018, due to the widespread use of antiretroviral therapies, the number of new HIV infections fell by 37%, and the number of HIV-related deaths fell by 45%, thus successfully saving a large number of lives. By the end of 2018, more than 23.3 million patients received antiviral treatments [3]. Based on this positive development, the Joint United Nations Programme on HIV/AIDS (UNAIDS) proposed the 90-90-90 goal at the United Nations General Assembly, which aims to achieve three core indicators : 90% of infected people know their viral status, 90% of diagnosed people receive continuous treatment, and 90% of treated people achieve viral load suppression. At the same time, the UNAIDS has set an ambitious goal of eliminating the AIDS epidemic by 2030, thus injecting new impetus into global health [3].

Mathematical models can predict the number of cases under both optimal and adverse scenarios when the progression of a disease is uncertain. Additionally, they are useful to evaluate the impact of preventive measures. Numerous scholars have been interested in analyzing the effects of HIV/AIDS via mathematical modeling (for example, see [4–6] and the references therein). For example, Huo et al. [4] proposed a novel class of HIV/AIDS transmission dynamic models, which integrates the bilinear incidence rate $\beta S I$ and therapeutic intervention strategies. They conducted a stability analysis of the disease based on the basic reproduction number R_0, and revealed that the disease would become extinct in the population when $R_0 < 1$, and would persist when $R_0 > 1$. Furthermore, they concluded that the disease could be eradicated by sufficiently increasing the treatment rate during the onset of the disease. Given the significance of incidence rates in infectious disease modeling, Jia et al. [5] extended the model by replacing the original bilinear incidence rate with a generalized nonlinear incidence rate $S g(I)$ and performed a systematic stability analysis of the modified model. Building upon this, S. Mangal et al. [6] introduced a category of undiagnosed HIV-infected individuals (E) and considered two transmission mechanisms, the bilinear incidence rate $(1 - w)\beta S E$ and the saturated incidence rate $\beta S I/(1 + uI)$, thereby investigating the inhibitory effects of preventive measures taken by both undiagnosed and confirmed HIV-infected individuals on the spread of the epidemic. In addition, numerous studies have also focused on spatial heterogeneity or environmental factors [20–22].

The incidence of a disease, defined as the number of new cases per unit time, is a critical factor in the modeling of epidemic dynamics. Many epidemic models commonly employ two types of incidence rates: the bilinear form $\beta S I$, where β represents the transmission rate, which quantifies the infectious potential of the disease [7, 8]; and the standard incidence rate $\frac{\beta S I}{N}$, where N denotes the total population size [9, 10]. However, the bilinear incidence rate often encounters significant limitations and challenges in accurately describing the spread of infectious diseases among human. To address this, a nonlinear incidence rate, which better captures the dynamics of disease transmission, has been proposed to replace the bilinear rate. The concept of nonlinear incidence rates was first introduced by Capasso and Serio [11] during their analysis on the cholera outbreak in Brai in 1973. They observed that the incidence rate did not proportionally increase with the number of infectious individuals I, but rather exhibited a slower growth as I rose. This led to the formulation of the saturated incidence rate $\frac{\beta S I}{1+\alpha I}$, which aligned well with the observed data. Here, the parameter α reprents inhibitory effects, such as overcrowding or changes in the behavior of susceptible individuals as the number of cases increase. Since then, numerous researchers have developed and analyzed epidemiological models that incorporated various forms of nonlinear incidence rates; for example, see [5, 12, 13].

Since most biological processes involve memory effects, the standard derivative becomes inadequate to accurately capture the transmission dynamics of infectious diseases, as it fails to incorporate memory. Therefore, an alternative form of the derivative—known as the fractional derivative—is employed, which accounts for this memory effect. In recent years, fractional calculus has gained significant attention across various research fields due to its ability to develop novel and accurate models [14, 15, 19]. The following key advantages distinguish these models from classical integer-order approaches:

(1) Improved Accuracy in Capturing Complex Dynamics: Fractional derivatives naturally incorporate memory effects and long-range dependencies, thus enabling a more precise representation of real-world transmission patterns—such as delayed impacts of past infections or interventions—that are often inadequately described by traditional models. This leads to more reliable predictions of outbreak trajectories and intervention outcomes.

(2) Flexibility in Modeling Heterogeneous Processes: Unlike integer-order models that assume instantaneous state transitions, fractional models can adapt to nonlinear and non-stationary data (e.g., spatially varying transmission rates or temporally evolving contact patterns). This flexibility allows for an improved alignment with empirical observations across diverse populations.

(3) Early Outbreak Detection and Forecasting: The memory-aware structure of fractional operators helps identify persistent or anti-persistent trends in early-phase data. By analyzing the Hurst exponent (reflecting long-term dependency), these models can detect emerging outbreaks earlier than classical methods, which enables timely public health responses.

(4) Explicit Representation of Memory Effects: Fractional calculus accounts for historical influences to the disease spread, such as immunity duration, incubation periods, or cumulative intervention impacts. This avoids the oversimplification of Markovian assumptions and provides a biologically realistic framework for diseases such as COVID-19 and tuberculosis.

(5) Enhanced Policy Evaluation and Optimization: Fractional models allow robust testing of control strategies (e.g., quarantine, vaccination) by simulating how memory-dependent dynamics interact with policies over time. This supports the design of cost-effective, context-specific interventions.

In light of the discussion above, this article presents a fractional-order model of the transmission dynamics of HIV/AIDS epidemic model with generalized incidence rates $f(S, I)$ and $g(S, E)$, which is inspired by the incidence rate given in [5, 6, 23]. This paper seeks to investigate the stability of a fractional-order HIV/AIDS model with a generalized nonlinear incidence rate. The objectives of this work are as follows:

- Establish the conditions for the existence of equilibrium points and derive the criteria for their local and global stability. Additionally, provide a supplementary proof of the global stability for the model presented in [6].

- Investigate the prediction and control of the HIV epidemic in Mexico, thereby focusing on the impact of the preventive measures taken by susceptible individuals and both undiagnosed or confirmed infected individuals on disease transmission.

The structure of this paper is organized as follows: Section 2 provides fundamental definitions and key results related to fractional-order derivatives; Section 3 formulates the frational-order model, examines the existence, uniqueness, positivity, and boundedness of its solutions, derives the basic reproduction number, and analyzes the local and global stability of equilibrium points; Section 4 explores the prediction and control of the HIV epidemic in Mexico, thereby considering two particular infection forms; and finally, Section 5 proposes the conclusion.

2. Preliminaries

In this section, we recall some fundamental concepts of fractional differential calculus, where the derivative is considered in the Caputo sense due to its significant memory effects, which are essential to accurately describe epidemic modeling dynamics. A key advantage of the Caputo fractional derivative is that the initial conditions for fractional differential equations retain the same form as those for integer-order differential equations. Moreover, the Caputo derivative of a constant is zero, which aligns with classical calculus and facilitates physical interpretation in modeling contexts.

Definition 2.1. ([24]) Let $g(t) \in L^1([t_0, \tau])$, where L^1 is the set of Lebesgue integrable functions; then, the left and right Riemann-Liouville (RL) integrals of a fractional-order α of the function $g(t)$ are given as follows:

$$ {}^{RL}_{t_0}I^{\alpha}_{t} g(t) = \frac{1}{\Gamma(\alpha)} \int_{t_0}^{t} (t-x)^{\alpha-1} g(x)dx, $$

and

$$ {}^{RL}_{t}I^{\alpha}_{\tau} g(t) = \frac{1}{\Gamma(\alpha)} \int_{t}^{\tau} (x-t)^{\alpha-1} g(x)dx $$

respectively, where $\Gamma(.)$ is the well-known gamma function.

Definition 2.2. ([24]) The left and right RL fractional-order derivatives of the function $g(t)$ are defined as follows:

$$ {}^{RL}_{t_0}D^{\alpha}_{t} g(t) = \frac{1}{\Gamma(n-\alpha)} \left(\frac{d}{dt}\right)^n \int_{t_0}^{t} (t-x)^{n-\alpha-1} g(x)dx, $$

and

$$ {}^{RL}_{t}D^{\alpha}_{\tau} g(t) = \frac{1}{\Gamma(n-\alpha)} \left(\frac{d}{dt}\right)^n \int_{t}^{\tau} (x-t)^{n-\alpha-1} g(x)dx $$

respectively, where n is any positive integer such that $n-1 < \alpha \leq n$.

Definition 2.3. ([24]) Let $g(t) \in C^n(t_0, \tau)$ (i.e., $g^{(n-1)}(t)$ is absolutely continuous); then, the left and right Caputo derivatives of a fractional-order α of the function $g(t)$ are defined as follows:

$$ {}^{C}_{t_0}D^{\alpha}_{t} g(t) = \frac{1}{\Gamma(n-\alpha)} \int_{t_0}^{t} (t-x)^{n-\alpha-1} g^{(n)}(x)dx, $$

and

$$ {}^{C}_{t}D^{\alpha}_{\tau} g(t) = \frac{(-1)^n}{\Gamma(n-\alpha)} \int_{t}^{\tau} (x-t)^{n-\alpha-1} g^{(n)}(x)dx $$

respectively, where n is any positive integer such that $n-1<\alpha\leq n$.

Lemma 2.4. *([25]) Let $f(x)\in C[a,b]$ and ${}_a^cD_x^\alpha f(x)\in C(a,b]$ for $0<\alpha\leq 1$; then,*

$$f(x)=f(a)+\frac{1}{\Gamma(\alpha)}({}_a^cD_x^\alpha g)(\xi)(x-a)^\alpha$$

with $a\leq\xi\leq x$, $\forall x\in(a,b]$.

Using Lemma 2.1, we state the following corollary.

Corollary 2.5. *([25]) Suppose that $g(x)\in C[0,b]$ and ${}_0^cD_x^\alpha g(x)\in C(0,b]$ for $0<\alpha\leq 1$. If ${}_0^cD_x^\alpha g(x)\geq 0$ $\forall t\in(0,b)$, then the function g is non-decreasing, and if ${}_0^cD_x^\alpha g(x)\leq 0$ $\forall x\in(0,b)$, then the function g is non-increasing for all $x\in(0,b)$.*

Lemma 2.6. *([26]) Let $\alpha\in(0,1)$, and consider a continuous function $x:[t_0,\infty)\to\mathbb{R}$ which satisfies the following condition:*

$${}_0^cD_t^\alpha x(t)+\mu x(t)\leq\nu, t\geq t_0,\mu,\nu\in\mathbb{R},\mu\neq 0.$$

Then, we have the inequality

$$x(t)\leq\left(x\left(t_0\right)-\frac{\nu}{\mu}\right)E_\alpha\left(-\mu\left(t-t_0\right)^\alpha\right)+\frac{\nu}{\mu},$$

for all $t\geq t_0$, where E_α is the Mittag-Leffler function of one parameter defined by

$$E_\alpha(t)=\sum_{k=0}^{\infty}\frac{t^k}{\Gamma(\alpha k+1)}.$$

Definition 2.7. ([27]) Let $F(s)$ be the Laplace transform of the $f(t)$. Then,

$$\mathcal{L}\{{}_0^cD_t^\alpha f(t),s\}=s^\alpha F(s)-\sum_{i=0}^{n-1}s^{\alpha-i-1}f^{(i)}(0),\alpha\in(n-1,n];n\in\mathbb{N}.$$

Definition 2.8. ([28]) The Mittag-Leffler function $E_{l,m}(x)$ is given by

$$E_{l,m}(x)=\sum_{n=0}^{\infty}\frac{x^n}{\Gamma(ln+m)},x\in\mathbb{R},l>0,m>0,$$

and satisfies the property

$$E_{l,m}(x)=xE_{l,l+m}(x)+\frac{1}{\Gamma(m)},$$

the Laplace transform of $t^{m-1}E_{l,m}\left(\pm\lambda t^l\right)$

$$\mathcal{L}\left[t^{m-1}E_{l,m}\left(\pm\lambda t^l\right)\right]=\frac{s^{l-m}}{s^l\mp\lambda}.$$

Lemma 2.9. *([10]) Let $0<\alpha<1$ and $g\in C[0,T]$ be a positive valued function. Then, for all $t\in[0,T)$, one has ${}_0^cD_t^\alpha(g(t)-g^*-g^*\ln\frac{g(t)}{g^*})\leq\left(1-\frac{g^*}{g(t)}\right){}_0^cD_t^\alpha g(t)$, for all $g*\in\mathbb{R}_+$.*

3. Fractional-order model formulation and analysis

In this section, we express the formulation of the HIV epidemic with a generalized nonlinear incidence rate and proceed with positivity and boundedness of the model. Additionally, the stability analysis of the model is included in this section.

3.1. Model formulation

In this section, we extend the model studied by S. Mangal et al. [6] to introduce the HIV/AIDS epidemic. The human population N is divided into the following six categories: Susceptible individuals (S), which represents people who have not yet been infected with HIV but may be infected with the virus; undiagnosed HIV-infected individuals (E), which represents people who have been infected with the HIV virus but have not yet been diagnosed through detecting due to their lack of awareness of their infection status, and may inadvertently play a critical role in the transmission chain; confirmed HIV-infected individuals (I), which represents people who have been confirmed to be infected with the HIV virus through HIV testing; treatment recipient (T); full-blown AIDS individuals (A), which represents people who no longer receive treatment; and low-risk individuals (R). Hence, the total population $N(t)$ is given by the following:

$$N(t) = S(t) + E(t) + I(t) + A(t) + T(t) + R(t).$$

The transmission dynamics of SEITAR HIV/AIDS model is governed by the following rules:

(A-1) The number of susceptible individuals (S) increases due to the births of newborns at a constant rate Λ and decreases due to natural morality at a rate μ;

(A-2) Diseases are transmitted in two forms, $f(S,I)$ and $g(S,E)$, which describe the interactions between susceptible individuals and both confirmed and undiagnosed infected individuals;

(A-3) Undiagnosed HIV-infected individuals (E) turn into the confirmed HIV-infected category (I) at a constant rate σ_1 based on diagnosis, while there is some direct progress to the full-blown AIDS category (A) at a constant rate σ_2 due to delayed diagnosis or lack of timely treatment;

(A-4) Confirmed HIV-infected individuals (I) move to the treatment category (T) at a rate k_1, though some of these individuals still convert to category (A) at a rate k_2 even after receiving treatment;

(A-5) Among the treated patients (T), some discontinue treatment due to financial constraints and return to the category (I) at a rate α_1, while another subset of patients, despite receiving treatment, progress to category (A) at a constant rate α_2; and

(A-6) The susceptible individuals (S) join the low-risk category (R) at a constant rate ξ.

Based on the transmission rules outlined aboved, our considered fractional-order SEITAR HIV/AIDS model is defined as follows:

$$\begin{cases} {}_0^cD_t^\alpha S = \Lambda^\alpha - f(S,I) - g(S,E) - (\xi^\alpha + \mu^\alpha)S, \\ {}_0^cD_t^\alpha E = f(S,I) + g(S,E) - (\sigma_1^\alpha + \sigma_2^\alpha + \mu^\alpha)\, E, \\ {}_0^cD_t^\alpha I = \sigma_1^\alpha E + \alpha_1^\alpha T - (k_1^\alpha + k_2^\alpha + \mu^\alpha)\, I, \\ {}_0^cD_t^\alpha T = k_1^\alpha I - (\alpha_1^\alpha + \alpha_2^\alpha + \delta_2^\alpha + \mu^\alpha)\, T, \\ {}_0^cD_t^\alpha A = \sigma_2^\alpha E + k_2^\alpha I + \alpha_2^\alpha T - (\delta_1^\alpha + \mu^\alpha)A, \\ {}_0^cD_t^\alpha R = \xi^\alpha S - \mu^\alpha R, \end{cases} \tag{3.1}$$

with the appropriate positive initial conditions

$$S(0) = S^0, E(0) = E^0, I(0) = I^0, T(0) = T^0, A(0) = A^0, R(0) = R^0,$$

where ${}_0^cD_t^\alpha$ is a Caputo fractional-order derivative, and $0 < \alpha \leqslant 1$. The epidemiological description of the parameters in the fractional-order SEITAR HIV/AIDS epidemic model (3.1) are shown in Table 1. The units of all parameters in Table 1 are year^{-1}.

Table 1. Parameters meaning of model (3.1).

Parameters	Epidemiological description
Λ	Recruitment rate
ξ	The proportion of people who develop safe habits in sexual contact rate
μ	Natural death rate
σ_1	Proportion of undiagnosed HIV-infected people who pass the test as confirmed infected
σ_2	The ratio from compartment E to compartment A due to delays in detection and treatment
α_1	The rate at which individuals receiving treatment leave compartment T and join I
α_2	The rate of developing into class A after receiving treatment
k_1	The rate of treatment for people with confirmed HIV
k_2	The ratio of diagnosed infected people to full-blown AIDS patient
δ_1	Disease-induced death rate for individuals in compartment A
δ_2	Disease-induced death rate for individuals in compartment T

3.2. *Positivity and boundedness*

In this subsection, we demonstrate that the solutions of model (3.1) are non-negative and bounded for whatever the positive initial conditions. For this purpose, we assume that the generalized incidence principal functions $f(S, I)$ and $g(S, E)$ are nonnegative and continuously differentiable in the interior of R_+^2. The following assumptions in [30] will be useful in the sequel:

$(H_1): f(0, I) = 0, g(0, E) = 0, f(S, 0) = 0, g(S, 0) = 0, \forall S, I, E > 0,$

$(H_2): \frac{\partial f(S,0)}{\partial S} = \frac{\partial g(S,0)}{\partial S} = 0, \forall S > 0,$

$(H_3): 0 < \frac{\partial f(S,I)}{\partial S} \leq \theta_1, 0 < \frac{\partial g(S,E)}{\partial S} \leq \theta_2, \forall S, I, E > 0, \theta_1, \theta_2$ are constants,

$(H_4): 0 < \frac{\partial f(S,I)}{\partial I} \leq \frac{f(S,I)}{I}, 0 < \frac{\partial g(S,E)}{\partial E} \leq \frac{g(S,E)}{E}, \forall S, E, I > 0,$

$(H_5): \frac{\partial^2 f(S,I)}{\partial I^2} \leq 0, \frac{\partial^2 g(S,E)}{\partial E^2} \leq 0, \forall S, I, E \geq 0.$

The functions f and g include a number of especial incidence rates. For instance,

1) $f, g(x, y) = \beta x^p, p \geq 1$ [16].
2) $f, g(x, y) = (\beta - \frac{\beta_1 y}{m+y})x, \beta > \beta_1, m > 0$ [12, 29].
3) $f, g(x, y) = \frac{\beta x}{x+\alpha y}, \alpha > 0$ [31].
4) $f, g(x, y) = \frac{\beta x}{1+\alpha y^p}, \alpha > 0, 0 < p \leq 1$ [32].
5) $f, g(x, y) = \frac{\beta x}{1+\alpha_1 x+\alpha_2 y+\alpha_3 xy}, \alpha_1, \alpha_2, \alpha_3 \geq 0$ [30, 33, 34].

Theorem 3.1. *For any nonnegative initial condition* $X(0) = (S(0), E(0), I(0), T(0), A(0), R(0))^T$, *there is always a unique solution for model (3.1) on* $[0, +\infty)$.

Proof. Let $X(t) = (S(t), E(t), I(t), T(t), A(t), R(t))^T$. Model (3.1) can be written as follows:

$${}_0^cD_t^\alpha X(t) = F(X(t)), \forall t \geq 0,$$

where

$$F\left(X(t)\right)=\begin{pmatrix} \Lambda^{\alpha}-f(S,I)-g(S,E)-(\xi^{\alpha}+\mu^{\alpha})S \\ f(S,I)+g(S,E)-\left(\sigma_1^{\alpha}+\sigma_2^{\alpha}+\mu^{\alpha}\right)E \\ \sigma_1^{\alpha}E+\alpha_1^{\alpha}T-\left(k_1^{\alpha}+k_2^{\alpha}+\mu^{\alpha}\right)I \\ k_1^{\alpha}I-\left(\alpha_1^{\alpha}+\alpha_2^{\alpha}+\delta_2^{\alpha}+\mu^{\alpha}\right)T \\ \sigma_2^{\alpha}E+k_2^{\alpha}I+\alpha_2^{\alpha}T-(\delta_1^{\alpha}+\mu^{\alpha})A \\ \xi^{\alpha}S-\mu^{\alpha}R \end{pmatrix}.$$

Utilizing hypothesis (H3) and the Lagrange mean value theorem, we conclude that $f(S,I)\leq\theta_1 S$ and $g(S,E)\leq\theta_2 S$.

Let

$$Q_1=\begin{pmatrix} -(\xi^{\alpha}+\mu^{\alpha}) & 0 & 0 & 0 & 0 & 0 \\ 0 & -\left(\sigma_1^{\alpha}+\sigma_2^{\alpha}+\mu^{\alpha}\right) & 0 & 0 & 0 & 0 \\ 0 & \sigma_1^{\alpha} & -\left(k_1^{\alpha}+k_2^{\alpha}+\mu^{\alpha}\right) & \alpha_1^{\alpha} & 0 & 0 \\ 0 & 0 & k_1^{\alpha} & -\left(\alpha_1^{\alpha}+\alpha_2^{\alpha}+\delta_2^{\alpha}+\mu^{\alpha}\right) & 0 & 0 \\ 0 & \sigma_2^{\alpha} & k_2^{\alpha} & \alpha_2^{\alpha} & -(\delta_1^{\alpha}+\mu^{\alpha}) & 0 \\ \xi^{\alpha} & 0 & 0 & 0 & 0 & -\mu^{\alpha} \end{pmatrix},$$

$$Q_2=\begin{pmatrix} -(\theta_1+\theta_2) & 0 & 0 & 0 & 0 & 0 \\ (\theta_1+\theta_2) & 0 & 0 & 0 & 0 & 0 \\ 0 & 0 & 0 & 0 & 0 & 0 \\ 0 & 0 & 0 & 0 & 0 & 0 \\ 0 & 0 & 0 & 0 & 0 & 0 \\ 0 & 0 & 0 & 0 & 0 & 0 \end{pmatrix}, Q_0=\begin{pmatrix} \Lambda^{\alpha} \\ 0 \\ 0 \\ 0 \\ 0 \\ 0 \end{pmatrix}.$$

For model (3.1), one can obtain $\|F(X(t))\|\leq\|Q_0\|+(\|Q_1\|+\|Q_2\|)\|X\|$.
Thus, according to Lemma 4 in [35], model (3.1) has a unique solution on $[0,+\infty)$.

Consider the following set:

$$\Omega=\left\{(S,E,I,T,A,R)\in\mathbb{R}_+^6 : S\geq 0, E\geq 0, I\geq 0, T\geq 0, A\geq 0, R\geq 0\right\}.$$

Now, we prove that every solution of model (3.1) is non-negative and lies in Ω.

Theorem 3.2. *If the initial conditions of model (3.1) are in the region Ω, then all the possible solutions of the model are lying within in Ω.*

Proof. Using Lemma 2.1, we establish the positivity of the solutions as follows:

$$\begin{aligned} {}_0^cD_t^{\alpha}S|_{S=0}&=\Lambda^{\alpha}>0, \\ {}_0^cD_t^{\alpha}E|_{E=0}&=f(S,I)\geq 0, \\ {}_0^cD_t^{\alpha}I|_{I=0}&=\sigma_1^{\alpha}E+\alpha_1^{\alpha}T\geq 0, \\ {}_0^cD_t^{\alpha}T|_{T=0}&=k_1^{\alpha}I\geq 0, \\ {}_0^cD_t^{\alpha}A|_{A=0}&=\sigma_2^{\alpha}E+k_2^{\alpha}I+\alpha_2^{\alpha}T\geq 0, \\ {}_0^cD_t^{\alpha}R|_{R=0}&=\xi^{\alpha}S\geq 0. \end{aligned} \tag{3.2}$$

If $(S(0), E(0), I(0), T(0), A(0), R(0)) \in \Omega$, due to (3.2) and Corollary 2.1, then one can deduce that the solution $(S(t), E(t), I(t), T(t), A(t), R(t))$ belongs to the hyperplanes of $S = 0, E = 0, I = 0, T = 0, A = 0$, and $R = 0$. Additionally, the vector field of each of these hyperplanes are included by Ω. It means that the solution of the fractional order model (3.1) is nonnegative.
Next, we prove the boundedness of the solution.
Summing all equations in model (3.1) leads to the following:

$$ {}_{0}^{c}D_{t}^{\alpha}N(t) \le \Lambda^{\alpha} - \mu^{\alpha}N(t). \tag{3.3} $$

Taking the Laplace transform into (3.3) leads to the following:

$$ \begin{aligned} S^{\alpha}L[N(t)] - S^{\alpha-1}N(0) &\le S^{-1}\Lambda^{\alpha} - \mu^{\alpha}L[N(t)], \\ L[N(t)] &\le \frac{s^{\alpha-1}}{s^{\alpha}+\mu^{\alpha}}N(0) + \frac{s^{-1}}{s^{\alpha}+\mu^{\alpha}}\Lambda^{\alpha}. \end{aligned} $$

Applying the Laplace inverse transform yields the following:

$$ N(t) \le L^{-1}\left[\tfrac{s^{\alpha-1}}{s^{\alpha}+\mu^{\alpha}}N(0)\right] + L^{-1}\left[\tfrac{s^{-1}}{s^{\alpha}+\mu^{\alpha}}\Lambda^{\alpha}\right] = N(0)E_{\alpha,1}\left(-\mu^{\alpha}t^{\alpha}\right) + \Lambda^{\alpha}t^{\alpha}E_{\alpha,\alpha+1}\left(-\mu^{\alpha}t^{\alpha}\right). $$

Let $N(0) \le \frac{\Lambda^{\alpha}}{\mu^{\alpha}}$; then, we gain $N(t) \le \frac{\Lambda^{\alpha}}{\mu^{\alpha}}\left[E_{\alpha,1}(-\mu^{\alpha}t^{\alpha}) + \mu^{\alpha}t^{\alpha}E_{\alpha,\alpha+1}(-\mu^{\alpha}t^{\alpha})\right] = \frac{\Lambda^{\alpha}}{\mu^{\alpha}}\frac{1}{\Gamma(1)} = \frac{\Lambda^{\alpha}}{\mu^{\alpha}}$.
Hence, the solutions of model (3.1) are non-negative and ultimately bounded.

3.3. *Equilibrium points stability*

In this section, we will derive all possible equilibrium points and compute the basic reproduction number by the next-generation matrix method, which is later shown in the graphical results with different effects. Moreover, we establish the local and global stability theories of equilibrium points for the fractional-order model (3.1).

3.3.1. Disease-free equilibrium (DFE)

Since the first four equations of the model are independent of A and R, to simplify the model analysis, consider the following subsystems:

$$ \begin{cases} {}_{0}^{c}D_{t}^{\alpha}S = \Lambda^{\alpha} - f(S,I) - g(S,E) - (\xi^{\alpha} + \mu^{\alpha})S, \\ {}_{0}^{c}D_{t}^{\alpha}E = f(S,I) + g(S,E) - \left(\sigma_1^{\alpha} + \sigma_2^{\alpha} + \mu^{\alpha}\right)E, \\ {}_{0}^{c}D_{t}^{\alpha}I = \sigma_1^{\alpha}E + \alpha_1^{\alpha}T - \left(k_1^{\alpha} + k_2^{\alpha} + \mu^{\alpha}\right)I, \\ {}_{0}^{c}D_{t}^{\alpha}T = k_2^{\alpha}I - \left(\alpha_1^{\alpha} + \alpha_2^{\alpha} + \delta_2^{\alpha} + \mu^{\alpha}\right)T, \end{cases} \tag{3.4} $$

with the non-negative initial condition as follows: $S(0) = S^0, E(0) = E^0, I(0) = I^0, T(0) = T^0$.

In the absence of disease, that is, $(E \equiv 0, I \equiv 0, T \equiv 0)$, model (3.4) admits a unique disease-free equilibrium (DFE) $P_0(S_0, E_0, I_0, T_0) = P_0\left(\frac{\Lambda^{\alpha}}{\xi^{\alpha}+\mu^{\alpha}}, 0, 0, 0\right)$. In order to derive the existence and uniqueness of the endemic equilibrium $P_*(S_*, E_*, I_*, T_*)$, we first compute the basic reproduction number of the model (3.4). For this purpose, we use the next generation matrix technique [36].

Theorem 3.3. *The basic reproduction number of model (3.4) takes the following form:* $R_0^{\alpha} = \frac{\frac{\partial g(S_0,0)}{\partial E}C + \frac{\partial f(S_0,0)}{\partial I}D}{C\left(\sigma_1^{\alpha}+\sigma_2^{\alpha}+\mu^{\alpha}\right)}$, *where* $C = \left(\alpha_1^{\alpha} + \alpha_2^{\alpha} + \delta_2^{\alpha} + \mu^{\alpha}\right)\left(k_2^{\alpha} + \mu^{\alpha}\right) + k_1^{\alpha}\left(\alpha_2^{\alpha} + \delta_2^{\alpha} + \mu^{\alpha}\right)$ *and* $D = \sigma_1^{\alpha}\left(\alpha_1^{\alpha} + \alpha_2^{\alpha} + \delta_2^{\alpha} + \mu^{\alpha}\right)$.

Proof. Let $X(t) = (E(t), I(t), T(t))^T$; then, model (3.4) can be written as follows:

$$\begin{cases} {}_0^cD_t^\alpha X = F(X) - V(X), \\ V(X) = V^-(X) - V^+(X), \end{cases}$$

where

$$F(X) = \begin{pmatrix} f(S, I) + g(S, E) \\ 0 \\ 0 \end{pmatrix}, V^+(X) = \begin{pmatrix} 0 \\ \sigma_1^\alpha E + \alpha_1^\alpha T \\ k_1^\alpha I \end{pmatrix}, V^-(X) = \begin{pmatrix} \left(\sigma_1^\alpha + \sigma_2^\alpha + \mu^\alpha\right) E \\ \left(k_1^\alpha + k_2^\alpha + \mu^\alpha\right) I \\ \left(\alpha_1^\alpha + \alpha_2^\alpha + \delta_2^\alpha + \mu^\alpha\right) T \end{pmatrix}.$$

$F(X)$ represents the occurrence rate of newly infected individuals in each compartment E, I, and T. $V^+(X)$ represents the rate at which individuals are transferred into compartments E, I, and T in a series of ways, and $V^-(X)$ represents the rate at which individuals are transferred out of compartments E, I, and T. Let f and ϑ be Jacobian matrices of $F(X)$ and $V(X)$ at E_0, respectively; then,

$$f = \begin{pmatrix} \frac{\partial g(S_0,0)}{\partial E} & \frac{\partial f(S_0,0)}{\partial I} & 0 \\ 0 & 0 & 0 \\ 0 & 0 & 0 \end{pmatrix}, \vartheta = \begin{pmatrix} \sigma_1^\alpha + \sigma_2^\alpha + \mu^\alpha & 0 & 0 \\ -\sigma_1^\alpha & k_1^\alpha + k_2^\alpha + \mu^\alpha & -\alpha_1^\alpha \\ 0 & -k_1^\alpha & \alpha_1^\alpha + \alpha_2^\alpha + \delta_2^\alpha + \mu^\alpha \end{pmatrix}.$$

The largest eigenvalue, namely the spectral radius of $f \cdot \vartheta^{-1}$, gives the R_0^α of model (3.4) as follows:

$$R_0^\alpha = \frac{\frac{\partial g(S_0,0)}{\partial E} C + \frac{\partial f(S_0,0)}{\partial I} D}{C\left(\sigma_1^\alpha + \sigma_2^\alpha + \mu^\alpha\right)}.$$

3.3.2. Endemic equilibrium point (EEP)

In this subsection, we provide the proof of existence and uniqueness of the endemic equilibrium point (EEP).

Theorem 3.4. *If $R_0^\alpha > 1$, then model (3.4) has a unique EEP $P_*(S_*, E_*, I_*, T_*)$.*

Proof. To obtain the equilibrium points of model (3.4), we have the following algebraic equations:

$$\begin{cases} \Lambda^\alpha - f(S, I) - g(S, E) - (\xi^\alpha + \mu^\alpha) S = 0, \\ f(S, I) + g(S, E) - (\sigma_1^\alpha + \sigma_2^\alpha + \mu^\alpha) E = 0, \\ \sigma_1^\alpha E + \alpha_1^\alpha T - (k_1^\alpha + k_2^\alpha + \mu^\alpha) I = 0, \\ k_1^\alpha I - (\alpha_1^\alpha + \alpha_2^\alpha + \delta_2^\alpha + \mu^\alpha) T = 0. \end{cases} \tag{3.5}$$

Calculating the above equalities, we reach $S = \frac{\Lambda^\alpha - \left(\sigma_1^\alpha + \sigma_2^\alpha + \mu^\alpha\right) E}{\xi^\alpha + \mu^\alpha}, I = \frac{D}{C} E, T = \frac{\sigma_1^\alpha k_1^\alpha}{C} E.$
By the second equation of model (3.5), we define the following:

$$\Phi(E) = f\left(\frac{\Lambda^\alpha - \left(\sigma_1^\alpha + \sigma_2^\alpha + \mu^\alpha\right) E}{\xi^\alpha + \mu^\alpha}, \frac{D}{C} E\right) + g\left(\frac{\Lambda^\alpha - \left(\sigma_1^\alpha + \sigma_2^\alpha + \mu^\alpha\right) E}{\xi^\alpha + \mu^\alpha}, E\right) - \left(\sigma_1^\alpha + \sigma_2^\alpha + \mu^\alpha\right) E.$$

Using assumption (H_1), we can deduce that $\Phi(0) = 0$ and $\Phi\left(\frac{\Lambda^\alpha}{\sigma_1^\alpha + \sigma_2^\alpha + \mu^\alpha}\right) = -\Lambda^\alpha < 0$.
Since the function $\Phi(E)$ is continuously differentiable with respect to the variable E in the interval

$\left[0, \frac{\Lambda^\alpha}{\sigma_1^\alpha+\sigma_2^\alpha+\mu^\alpha}\right]$, it can be further obtained that

$$\begin{aligned}\Phi'(E) = &-\frac{\sigma_1^\alpha+\sigma_2^\alpha+\mu^\alpha}{\xi^\alpha+\mu^\alpha}\frac{\partial f\left(\frac{\Lambda^\alpha-\left(\sigma_1^\alpha+\sigma_2^\alpha+\mu^\alpha\right)E}{\xi^\alpha+\mu^\alpha}, \frac{D}{C}E\right)}{\partial S} + \frac{D}{C}\frac{\partial f\left(\frac{\Lambda^\alpha-\left(\sigma_1^\alpha+\sigma_2^\alpha+\mu^\alpha\right)E}{\xi^\alpha+\mu^\alpha}, \frac{D}{C}E\right)}{\partial I}\\ &-\frac{\sigma_1^\alpha+\sigma_2^\alpha+\mu^\alpha}{\xi^\alpha+\mu^\alpha}\frac{\partial g\left(\frac{\Lambda^\alpha-\left(\sigma_1^\alpha+\sigma_2^\alpha+\mu^\alpha\right)E}{\xi^\alpha+\mu^\alpha}, E\right)}{\partial S} + \frac{\partial g\left(\frac{\Lambda^\alpha-\left(\sigma_1^\alpha+\sigma_2^\alpha+\mu^\alpha\right)E}{\xi^\alpha+\mu^\alpha}, E\right)}{\partial E} - \left(\sigma_1^\alpha+\sigma_2^\alpha+\mu^\alpha\right).\end{aligned}$$

If the function Φ satisfies $\Phi'(0) > 0$, then $\Phi(E) = 0$ admits at least one positive root E_* in the interval $\left(0, \frac{\Lambda^\alpha}{\sigma_1^\alpha+\sigma_2^\alpha+\mu^\alpha}\right]$.
By hypothesis (H_2), we see that

$$\begin{aligned}\Phi'(0) &= -\frac{\sigma_1^\alpha+\sigma_2^\alpha+\mu^\alpha}{\xi^\alpha+\mu^\alpha}\frac{\partial f\left(S_0,0\right)}{\partial S} + \frac{D}{C}\frac{\partial f\left(S_0,0\right)}{\partial I} - \frac{\sigma_1^\alpha+\sigma_2^\alpha+\mu^\alpha}{\xi^\alpha+\mu^\alpha}\frac{\partial g\left(S_0,0\right)}{\partial S} + \frac{\partial g\left(S_0,0\right)}{\partial E} - \left(\sigma_1^\alpha+\sigma_2^\alpha+\mu^\alpha\right)\\ &= \left(\sigma_1^\alpha+\sigma_2^\alpha+\mu^\alpha\right)\left(R_0^\alpha-1\right).\end{aligned}$$

Therefore, $R_0^\alpha > 1$ leads to $\Phi'(0) > 0$. Furthermore, model (3.4) has at least an EEP $P_*\left(S_*, E_*, I_*, T_*\right)$, where

$$S_* = \frac{\Lambda^\alpha - \left(\sigma_1^\alpha+\sigma_2^\alpha+\mu^\alpha\right)E_*}{\xi^\alpha+\mu^\alpha}, I_* = \frac{D}{C}E_*, T_* = \frac{\sigma_1^\alpha k_1^\alpha}{C}E_*.$$

Next,we will prove the uniqueness of the EEP. Substituting $P_*\left(S_*, E_*, I_*, T_*\right)$ into the second equation of model (3.5) yields the following:

$$\sigma_1^\alpha+\sigma_2^\alpha+\mu^\alpha = \frac{f\left(S_*, I_*\right)}{E_*} + \frac{g\left(S_*, E_*\right)}{E_*}.$$

Combing with the above equality, we obtain the following:

$$\begin{aligned}\Phi'(E_*) = &-\frac{\sigma_1^\alpha+\sigma_2^\alpha+\mu^\alpha}{\xi^\alpha+\mu^\alpha}\frac{\partial f\left(S_*, I_*\right)}{\partial S} - \frac{\sigma_1^\alpha+\sigma_2^\alpha+\mu^\alpha}{\xi^\alpha+\mu^\alpha}\frac{\partial g\left(S_*, E_*\right)}{\partial S} + \frac{D}{C}\left(\frac{\partial f(S_*, I_*)}{\partial I} - \frac{f(S_*, I_*)}{I_*}\right)\\ &+\left(\frac{\partial g(S_*, E_*)}{\partial E} - \frac{g(S_*, E_*)}{E_*}\right).\end{aligned}$$

Form hypothesis (H_4), it is easy to gain that $\Phi'(E_*) < 0$. We utilize the contradiction argument to drive the uniqueness of the EEP $P_*\left(S_*, E_*, I_*, T_*\right)$. Suppose there is an another EEP $P_{**}\left(S_{**}, E_{**}, I_{**}, T_{**}\right)$; after some simple calculations, it is easy to arrive that $\Phi'(E_{**}) > 0$, which is a contradiction. This concludes Theorem 3.4.

3.3.3. Local stability of DFE and EEP

The local stability analysis of the DFE P_0 and the EEP P_* of model (3.4) is established in this subsection.

Theorem 3.5. *If $R_0^\alpha < 1$, then the DFE P_0 is locally asymptotically stable(LAS).*

Proof. The Jacobian matrix of model (3.4) at P_0 is as follows:

$$J(P_0)=\begin{bmatrix} -\xi^{\alpha}-\mu^{\alpha} & -\frac{\partial g(S_0,0)}{\partial E} & -\frac{\partial f(S_0,0)}{\partial I} & 0 \\ 0 & \frac{\partial g(S_0,0)}{\partial E}-\left(\sigma_1^{\alpha}+\sigma_2^{\alpha}+\mu^{\alpha}\right) & \frac{\partial f(S_0,0)}{\partial I} & 0 \\ 0 & \sigma_1^{\alpha} & -\left(k_1^{\alpha}+k_2^{\alpha}+\mu^{\alpha}\right) & \alpha_1^{\alpha} \\ 0 & 0 & k_1^{\alpha} & -\left(\alpha_1^{\alpha}+\alpha_2^{\alpha}+\delta_2^{\alpha}+\mu^{\alpha}\right) \end{bmatrix}.$$

Take the characteristic equation $|\lambda E - J(P_0)| = (\lambda + \xi^{\alpha} + \mu^{\alpha})\, P(\lambda)$,
where

$$P(\lambda) = \lambda^3 + x_1\lambda^2 + x_2\lambda + x_3 = 0.$$

$$\begin{aligned} x_1 &= (k_1^{\alpha}+k_2^{\alpha}+\mu^{\alpha}+\alpha_1^{\alpha}+\alpha_2^{\alpha}+\delta_2^{\alpha}+\mu^{\alpha}) + (\sigma_1^{\alpha}+\sigma_2^{\alpha}+\mu^{\alpha}) - \frac{\partial g(S_0,0)}{\partial E}, \\ x_2 &= (k_1^{\alpha}+k_2^{\alpha}+\mu^{\alpha}+\alpha_1^{\alpha}+\alpha_2^{\alpha}+\delta_2^{\alpha}+\mu^{\alpha})\left[(\sigma_1^{\alpha}+\sigma_2^{\alpha}+\mu^{\alpha}) - \frac{\partial g(S_0,0)}{\partial E}\right] \\ &\quad + (k_1^{\alpha}+k_2^{\alpha}+\mu^{\alpha})(\alpha_1^{\alpha}+\alpha_2^{\alpha}+\delta_2^{\alpha}+\mu^{\alpha}) - \alpha_1^{\alpha}k_1^{\alpha} - \frac{\partial f(S_0,0)}{\partial I}\sigma_1^{\alpha}, \\ x_3 &= \left[(\sigma_1^{\alpha}+\sigma_2^{\alpha}+\mu^{\alpha}) - \frac{\partial g(S_0,0)}{\partial E}\right](k_1^{\alpha}+k_2^{\alpha}+\mu^{\alpha})(\alpha_1^{\alpha}+\alpha_2^{\alpha}+\delta_2^{\alpha}+\mu^{\alpha}) \\ &\quad - \frac{\partial f(S_0,0)}{\partial I}\sigma_1^{\alpha}(\alpha_1^{\alpha}+\alpha_2^{\alpha}+\delta_2^{\alpha}+\mu^{\alpha}) - \left[(\sigma_1^{\alpha}+\sigma_2^{\alpha}+\mu^{\alpha}) - \frac{\partial g(S_0,0)}{\partial E}\right]\alpha_1^{\alpha}k_1^{\alpha} \\ &= C(\sigma_1^{\alpha}+\sigma_2^{\alpha}+\mu^{\alpha})(1-R_0^{\alpha}). \end{aligned}$$

This indicates that if $R_0^{\alpha} < 1$, then $\left(\sigma_1^{\alpha}+\sigma_2^{\alpha}+\mu^{\alpha}\right) - \frac{\partial g(S_0,0)}{\partial E} > 0$ and $x_1, x_2, x_3, x_1x_2 - x_3 > 0$. By the Routh-Hurwitz criteria (see [6]), these conditions ensure the local asymptotical stability of the DFE P_0 of the fractional-order model (3.4) whenever $R_0^{\alpha} < 1$.

Now, we present the Fractional-Routh-Hurwitz criterion for a four-dimensional fractional-order system [37].
Let

$$P(\lambda) = \lambda^4 + a_1\lambda^3 + a_2\lambda^2 + a_3\lambda + a_4 = 0$$

be a characteristic equation of the jacobian matrix evaluated at the equilibrium point and

$$D(P(\lambda)) = H(P, P')$$

be the discriminant of $P(\lambda)$, where $H(P, P')$ is the resultant of P and its derivative P' as follows:

$$H(P,P') = \begin{vmatrix} 1 & a_1 & a_2 & a_3 & a_4 & 0 & 0 \\ 0 & 1 & a_1 & a_2 & a_3 & a_4 & 0 \\ 0 & 0 & 1 & a_1 & a_2 & a_3 & a_4 \\ 4 & 3a_1 & 2a_2 & a_3 & 0 & 0 & 0 \\ 0 & 4 & 3a_1 & 2a_2 & a_3 & 0 & 0 \\ 0 & 0 & 4 & 3a_1 & 2a_2 & a_3 & 0 \\ 0 & 0 & 0 & 4 & 3a_1 & 2a_2 & a_3 \end{vmatrix}.$$

Then,

$$\begin{aligned} D(P(\lambda)) = &(a_1a_2a_3)^2 - 4(a_1a_3)^3 + 18a_1a_2a_3^3 - 4a_1^2a_2^3a_4 - 6(a_1a_3)^2a_4 \\ &+ 144a_2a_3^2a_4 - 80a_1a_2^2a_3a_4 - 192a_1a_3a_4^2 + 18a_1^3a_2a_3a_4 + 144a_1^2a_2a_4^2 \\ &- 4a_2^3a_3^2 - 27a_3^4 - 27a_1^4a_4^2 - 128a_2^2a_4^2 + 16a_2^4a_4 + 256a_4^3. \end{aligned}$$

The fractional order Routh-Hurwitz criterion is as follows:

Case1. If $\alpha = 1$, then the necessary and sufficient conditions for an equilibrium point to be LAS are $H_1 > 0, H_2 > 0, H_3 = 0$, and $a_4 > 0$, where

$$H_1 = a_1, \quad H_2 = \begin{vmatrix} a_1 & 1 \\ a_3 & a_2 \end{vmatrix}, \quad H_3 = \begin{vmatrix} a_1 & 1 & 0 \\ a_3 & a_2 & a_1 \\ 0 & a_4 & a_3 \end{vmatrix}$$

are Routh-Hurwitz determinants. The above condition is sufficient but not necessary for an equilibrium point to be LAS when $\alpha \in [0, 1)$.

Case2. The equilibrium point is unstable for $\alpha > \frac{2}{3}$ when $D(P(\lambda)) > 0, a_1 > 0$, and $a_2 < 0$.

Case3. The equilibrium point is LAS for $\alpha < \frac{1}{3}$ when $D(P(\lambda)) < 0, a_1 > 0, a_3 > 0$, and $a_4 > 0$. Moreover, if $D(P(\lambda)) < 0, a_1 < 0, a_2 > 0, a_3 < 0$, and $a_4 > 0$, then the equilibrium point is unstable.

Case4. The equilibrium point is LAS for all $\alpha \in (0, 1)$ whenever $D(P(\lambda)) < 0, a_1 > 0, a_2 > 0, a_3 > 0, a_4 > 0$, and $a_2 = \frac{a_1 a_4}{a_3} + \frac{a_3}{a_1}$.

Case5. The necessary condition to be LAS for an equilibrium point is $a_4 > 0$.

To analyze the stability of the EEP, the Jacobian matrix at the EEP is defined and calculated as follows:

$$J(P_*) = \begin{bmatrix} a_{11} & a_{12} & a_{13} & 0 \\ a_{21} & a_{22} & a_{23} & 0 \\ 0 & a_{32} & a_{33} & a_{34} \\ 0 & 0 & a_{43} & a_{44} \end{bmatrix},$$

where

$$\begin{aligned}
a_{11} &= -\frac{\partial f(S_*, I_*)}{\partial S} - \frac{\partial g(S_*, E_*)}{\partial S} - (\xi^\alpha + \mu^\alpha), a_{12} = -\frac{\partial g(S_*, E_*)}{\partial E}, a_{13} = -\frac{\partial f(S_*, I_*)}{\partial I}, \\
a_{21} &= \frac{\partial f(S_*, E_*)}{\partial S} + \frac{\partial g(S_*, E_*)}{\partial S}, a_{22} = \frac{\partial g(S_*, E_*)}{\partial E_*} - (\sigma_1^\alpha + \sigma_2^\alpha + \mu^\alpha), a_{23} = \frac{\partial f(S_*, I_*)}{\partial I}, \\
a_{32} &= \sigma_1^\alpha, a_{33} = -(k_1^\alpha + k_2^\alpha + \mu^\alpha), a_{34} = \alpha_1^\alpha, \\
a_{43} &= k_1^\alpha, a_{44} = -(\alpha_1^\alpha + \alpha_2^\alpha + \delta_2^\alpha + \mu^\alpha).
\end{aligned}$$

Then, we obtain the characteristic polynomial of $J(P_*)$ as follows:

$$P(\lambda) = \lambda^4 + b_1\lambda^3 + b_2\lambda^2 + b_3\lambda + b_4,$$

where

$$\begin{aligned}
b_1 &= -(a_{11} + a_{22} + a_{33} + a_{44}), \\
b_2 &= a_{11}a_{22} - a_{12}^2 - a_{23}a_{32} - a_{34}a_{43} + (a_{11} + a_{22})(a_{33} + a_{44}), \\
b_3 &= a_{23}a_{32}(a_{11} + a_{44}) + a_{34}a_{43}(a_{11} + a_{22}) - a_{13}a_{21}a_{32} - (a_{33} + a_{44})\left(a_{11}a_{22} - a_{12}^2\right), \\
b_4 &= a_{13}a_{21}a_{32}a_{44} - a_{23}a_{32}a_{11}a_{44} - a_{34}a_{43}\left(a_{11}a_{22} - a_{12}^2\right).
\end{aligned}$$

Based on the discussion above, we present the following theorem.

Theorem 3.6. *If model (3.4) satisfies the Fractional-Routh-Hurwitz criteria, then the EEP P_* is LAS.*

3.3.4. Global stability of the DFE and EEP

In this subsection, we use the Lyapunov theorem to establish the global stability for the DFE P_0 and the EEP P_*.

Theorem 3.7. *If $R_0^\alpha < 1$, then the DFE P_0 is globally asymptotically stable (GAS) for any $\alpha \in (0,1]$.*

Proof. We construct a Lyapunov function as follows:

$$\varphi(t) = E(t) + \frac{\left(\sigma_1^\alpha+\sigma_2^\alpha+\mu^\alpha\right)\left(\frac{\partial f(S_0,0)}{\partial I}D\right)}{\sigma_1^\alpha\left(\frac{\partial g(S_0,0)}{\partial E}C+\frac{\partial f(S_0,0)}{\partial I}D\right)}I(t) + \frac{\alpha_1^\alpha\left(\sigma_1^\alpha+\sigma_2^\alpha+\mu^\alpha\right)\left(\frac{\partial f(S_0,0)}{\partial I}D\right)}{\sigma_1^\alpha\left(\alpha_1^\alpha+\alpha_2^\alpha+\delta_2^\alpha+\mu^\alpha\right)\left(\frac{\partial g(S_0,0)}{\partial E}C+\frac{\partial f(S_0,0)}{\partial I}D\right)}T(t).$$

Applying the Caputo fractional derivative on $\varphi(t)$, we have the following:

$${}_0^cD_t^\alpha\varphi(t) = {}_0^cD_t^\alpha E(t)+\frac{\left(\sigma_1^\alpha+\sigma_2^\alpha+\mu^\alpha\right)\left(\frac{\partial f(S_0,0)}{\partial I}D\right){}_0^cD_t^\alpha I(t)}{\sigma_1^\alpha\left(\frac{\partial g(S_0,0)}{\partial E}C+\frac{\partial f(S_0,0)}{\partial I}D\right)}+\frac{\alpha_1^\alpha\left(\sigma_1^\alpha+\sigma_2^\alpha+\mu^\alpha\right)\left(\frac{\partial f(S_0,0)}{\partial I}D\right){}_0^cD_t^\alpha T(t)}{\sigma_1^\alpha\left(\alpha_1^\alpha+\alpha_2^\alpha+\delta_2^\alpha+\mu^\alpha\right)\left(\frac{\partial g(S_0,0)}{\partial E}C+\frac{\partial f(S_0,0)}{\partial I}D\right)}.$$

After some simple calculations, we have the following:

$$\begin{aligned}
{}_0^cD_t^\alpha\varphi(t) &= f(S,I)+g(S,E)-\left(\sigma_1^\alpha+\sigma_2^\alpha+\mu^\alpha\right)E+\frac{\left(\sigma_1^\alpha+\sigma_2^\alpha+\mu^\alpha\right)\left(\frac{\partial f(S_0,0)}{\partial I}D\right)}{\sigma_1^\alpha\left(\frac{\partial g(S_0,0)}{\partial E}C+\frac{\partial f(S_0,0)}{\partial I}D\right)}[\sigma_1^\alpha E+\alpha_1^\alpha T- \\
&\quad (k_1^\alpha+k_2^\alpha+\mu^\alpha)I]+\frac{\alpha_1^\alpha\left(\sigma_1^\alpha+\sigma_2^\alpha+\mu^\alpha\right)\left(\frac{\partial f(S_0,0)}{\partial I}D\right)}{\sigma_1^\alpha\left(\alpha_1^\alpha+\alpha_2^\alpha+\delta_2^\alpha+\mu^\alpha\right)\left(\frac{\partial g(S_0,0)}{\partial E}C+\frac{\partial f(S_0,0)}{\partial I}D\right)}\left(k_1^\alpha I-\left(\alpha_1^\alpha+\alpha_2^\alpha+\delta_2^\alpha+\mu^\alpha\right)T\right) \\
&= f(S,I)+g(S,E)-\left(\sigma_1^\alpha+\sigma_2^\alpha+\mu^\alpha\right)E+\frac{\left(\sigma_1^\alpha+\sigma_2^\alpha+\mu^\alpha\right)\left(\frac{\partial f(S_0,0)}{\partial I}D\right)}{\frac{\partial g(S_0,0)}{\partial E}C+\frac{\partial f(S_0,0)}{\partial I}D}\left(E-\frac{k_1^\alpha+k_2^\alpha+\mu^\alpha}{\sigma_1^\alpha}I\right. \\
&\quad \left.+\frac{\alpha_1^\alpha}{\sigma_1^\alpha}T\right)+\frac{\left(\sigma_1^\alpha+\sigma_2^\alpha+\mu^\alpha\right)\frac{\partial f(S_0,0)}{\partial I}D}{\frac{\partial g(S_0,0)}{\partial E}C+\frac{\partial f(S_0,0)}{\partial I}D}\left(\frac{\alpha_1^\alpha k_1^\alpha}{\sigma_1\left(\alpha_1^\alpha+\alpha_2^\alpha+\delta_2^\alpha+\mu^\alpha\right)}I-\frac{\alpha_1^\alpha}{\sigma_1^\alpha}T\right) \\
&= f(S,I)+g(S,E)-\left(\sigma_1^\alpha+\sigma_2^\alpha+\mu^\alpha\right)E+\frac{\left(\sigma_1^\alpha+\sigma_2^\alpha+\mu^\alpha\right)\frac{\partial f(S_0,0)}{\partial I}D}{\frac{\partial g(S_0,0)}{\partial E}C+\frac{\partial f(S_0,0)}{\partial I}D}\left(E-\frac{C}{D}I\right) \\
&= f(S,I)+g(S,E)-\frac{\left(\sigma_1^\alpha+\sigma_2^\alpha+\mu^\alpha\right)C}{\frac{\partial g(S_0,0)}{\partial E}C+\frac{\partial f(S_0,0)}{\partial I}D}\left(\frac{\partial g(S_0,0)}{\partial E}E+\frac{\partial f(S_0,0)}{\partial I}I\right).
\end{aligned}$$

From the first equation of model (3.4), it can be concluded that ${}_0^cD_t^\alpha S(t) \le \Lambda^\alpha-(\xi^\alpha+\mu^\alpha)S(t)$. According to Lemma 2.2, there is $S(t) \le \left(S_0-\frac{\Lambda^\alpha}{\xi^\alpha+\mu^\alpha}\right)E_\alpha\left(-(\xi^\alpha+\mu^\alpha)t^\alpha\right)+\frac{\Lambda^\alpha}{\xi^\alpha+\mu^\alpha}$, which means $\lim_{t\to+\infty} supS(t) \le \frac{\Lambda^\alpha}{\xi^\alpha+\mu^\alpha} = S_0$. According to hypothetical conditions (H_3) and (H_5), we obtain the following:

$$f(S,I) \le \frac{\partial f(S_0,0)}{\partial I}I, g(S,E) \le \frac{\partial g(S_0,0)}{\partial E}E.$$

Thus,

$${}_0^cD_t^\alpha\varphi(t) \le \left(\frac{\partial g(S_0,0)}{\partial E}E+\frac{\partial f(S_0,0)}{\partial I}I\right)\left(1-\frac{1}{R_0^\alpha}\right).$$

Therefore, when $R_0^\alpha < 1$ holds, we have ${}_0^cD_t^\alpha\varphi(t) \le 0$. Furthermore, it is easy to verify that the single point set $\{P_0\}$ is the largest compact invariant set of $\left\{(S, E, I, T) \in R_4^+ : {}_0^cD_t^\alpha\varphi(t) = 0\right\}$. According to the fractional LaSalle's invariance principle, we can reach the following conclusion: If $R_0^\alpha < 1$, then the DFE P_0 is GAS for any $\alpha \in (0, 1]$.

Theorem 3.8. *If $R_0^\alpha > 1$ and inequalities (H_6) and (H_7) are true, then for any $\alpha \in (0, 1]$, the EEP P_* is GAS, where*

$$(H_6)\left(1-\frac{f(S,I_*)}{f(S,I)}\right)\left(\frac{f(S,I)}{f(S,I_*)}-\frac{I}{I_*}\right) \le 0,\ \forall S, E, I > 0,$$
$$(H_7)\left(1-\frac{f(S,I_*)g(S_*,E_*)}{f(S_*,I_*)g(S,E)}\right)\left(\frac{f(S_*,I_*)g(S,E)}{f(S,I_*)g(S_*,E_*)}-\frac{E}{E_*}\right) \le 0,\ \forall S, E, I > 0.$$

Proof. Define the Lyapunov function $\Psi(t)$ as follows:

$$\Psi(t) = \left(S(t) - S_* - \int_{S_*}^{S(t)} \frac{f(S_*, I_*)}{f(\theta, I_*)} d\theta\right) + \left(E(t) - E_* - \int_{E_*}^{E(t)} \frac{E_*}{\theta} d\theta\right) + \frac{f(S_* I_*)}{\sigma_1^\alpha E_*}\left(I(t) - I_* - \int_{I_*}^{I(t)} \frac{I_*}{\theta} d\theta\right)$$
$$+ \frac{\alpha_1^\alpha f(S_*, I_*)}{\sigma_1^\alpha\left(\alpha_1^\alpha + \alpha_2^\alpha + \delta_2^\alpha + \mu^\alpha\right)E_*}\left(T(t) - T_* - \int_{T_*}^{T(t)} \frac{T_*}{\theta} d\theta\right).$$

The fractional derivative of $\Psi(t)$ satisfies the following:

$${}_0^cD_t^\alpha\Psi(t) \le \left(1 - \frac{f(S_*, I_*)}{f(S, I_*)}\right){}_0^cD_t^\alpha S(t) + \left(1 - \frac{E_*}{E}\right){}_0^cD_t^\alpha E(t) + \frac{f(S_*, I_*)}{\sigma_1^\alpha E_*}\left(1 - \frac{I_*}{I}\right){}_0^cD_t^\alpha I(t)$$
$$+ \frac{\alpha_1^\alpha f(S_*, I_*)}{\sigma_1^\alpha\left(\alpha_1^\alpha + \alpha_2^\alpha + \delta_2^\alpha + \mu^\alpha\right)E_*}\left(1 - \frac{T_*}{T}\right){}_0^cD_t^\alpha T(t).$$

Using the first equation of model (3.4), we obtain the following:

$$\left(1 - \frac{f(S_*, I_*)}{f(S, I_*)}\right){}_0^cD_t^\alpha S(t) = \left(1 - \frac{f(S_*, I_*)}{f(S, I_*)}\right)\left(\Lambda^\alpha - f(S, I) - g(S, E) - (\xi^\alpha + \mu^\alpha) S\right).$$

By substituting $\Lambda^\alpha = f(S_*, I_*) + g(S_*, E_*) + (\xi^\alpha + \mu^\alpha) S_*$ in the above equation, we obtain the following:

$$\begin{aligned}\left(1 - \frac{f(S_*, I_*)}{f(S, I_*)}\right){}_0^cD_t^\alpha S(t) &= (\xi^\alpha + \mu^\alpha)\left(1 - \frac{f(S_*, I_*)}{f(S, I_*)}\right)(S_* - S)\\ &\quad + f(S_*, I_*)\left(1 - \frac{f(S_*, I_*)}{f(S, I_*)} - \frac{f(S, I)}{f(S_*, I_*)} + \frac{f(S, I)}{f(S, I_*)}\right)\\ &\quad + g(S_*, E_*)\left(1 - \frac{f(S_*, I_*)}{f(S, I_*)} - \frac{g(S, E)}{g(S_*, E_*)} + \frac{f(S_*, I_*)\, g(S, E)}{f(S, I_*)\, g(S_*, E_*)}\right).\end{aligned} \tag{3.6}$$

From the second equation of model (3.4), we have the following:

$$\left(1 - \frac{E_*}{E}\right){}_0^cD_t^\alpha E(t) = \left(1 - \frac{E_*}{E}\right)\left(f(S, I) + g(S, E) - (\sigma_1^\alpha + \sigma_2^\alpha + \mu^\alpha) E\right).$$

By means of the equalities $\sigma_1^\alpha + \sigma_2^\alpha + \mu^\alpha = \frac{f(S_*,I_*)}{E_*} + \frac{g(S_*,E_*)}{E_*}$, we gain the following:

$$\begin{aligned}\left(1 - \frac{E_*}{E}\right){}_0^cD_t^\alpha E(t) &= f(S_*, I_*)\left(1 - \frac{f(S, I)E_*}{f(S_*, I_*)\, E} - \frac{E}{E_*} + \frac{f(S, I)}{f(S_*, I_*)}\right)\\ &\quad + g(S_*, I_*)\left(1 - \frac{g(S, E)E_*}{g(S_*, E_*)\, E} - \frac{E}{E_*} + \frac{g(S, E)}{g(S_*, E_*)}\right).\end{aligned} \tag{3.7}$$

By the third equation of model (3.4), we obtain the following:

$$\frac{f(S_*, E_*)}{\sigma_1^\alpha E_*}\left(1-\frac{I_*}{I}\right){}_0^cD_t^\alpha I(t) = \frac{f(S_*, I_*)}{\sigma_1^\alpha E_*}\left(1-\frac{I_*}{I}\right)(\sigma_1^\alpha E + \alpha_1^\alpha T - (k_1^\alpha + k_2^\alpha + \mu^\alpha) I).$$

By substituting $I_* = \frac{\sigma_1^\alpha E_* + \alpha_1^\alpha T_*}{k_1^\alpha + k_1^\alpha + \mu^\alpha}$ and $I_* = \frac{\alpha_1^\alpha + \alpha_2^\alpha + \delta_2^\alpha + \mu^\alpha}{k_1^\alpha} T_*$ into the above equation, we deduce the following:

$$\begin{aligned}\frac{f(S_*, I_*)}{\sigma_1^\alpha E_*}\left(1-\frac{I_*}{I}\right){}_0^cD_t^\alpha I(t) &= f(S_*, I_*)\left(1+\frac{E}{E_*}-\frac{I_*E}{IE_*}-\frac{I}{I_*}\right)\\ &+ f(S_*, I_*)\left(\frac{\alpha_1^\alpha T}{\sigma_1^\alpha E_*} - \frac{\alpha_1^\alpha\left(\alpha_1^\alpha+\alpha_2^\alpha+\delta_2^\alpha+\mu^\alpha\right)T_*T}{\sigma_1^\alpha k_1^\alpha E_* I} - \frac{\alpha_1^\alpha k_1^\alpha I}{\sigma_1^\alpha\left(\alpha_1^\alpha+\alpha_2^\alpha+\delta_2^\alpha+\mu^\alpha\right)E_*} + \frac{\alpha_1^\alpha T_*}{\sigma_1^\alpha E_*}\right).\end{aligned} \tag{3.8}$$

By observing the fourth equation of model (3.4), we see that

$$\frac{\alpha_1^\alpha f(S_*, I_*)}{\sigma_1^\alpha\left(\alpha_1^\alpha+\alpha_2^\alpha+\delta_2^\alpha+\mu^\alpha\right)E_*}\left(1-\frac{T_*}{T}\right){}_0^cD_t^\alpha T(t) = \frac{\alpha_1^\alpha f(S_*, I_*)\left(k_1^\alpha I - \left(\alpha_1^\alpha+\alpha_2^\alpha+\delta_2^\alpha+\mu^\alpha\right)T\right)}{\sigma_1^\alpha\left(\alpha_1^\alpha+\alpha_2^\alpha+\delta_2^\alpha+\mu^\alpha\right)E_*}\left(1-\frac{T_*}{T}\right).$$

Inserting $\alpha_1^\alpha + \alpha_2^\alpha + \delta_2^\alpha + \mu^\alpha = \frac{k_1^\alpha I_*}{T_*}$ into the above equation, we derive the following:

$$\begin{aligned}\frac{\alpha_1^\alpha f(S_*, I_*)}{\sigma_1^\alpha\left(\alpha_1^\alpha+\alpha_2^\alpha+\delta_2^\alpha+\mu^\alpha\right)E_*}\left(1-\frac{T_*}{T}\right){}_0^cD_t^\alpha T(t) &= f(S_*, I_*)\frac{\alpha_1^\alpha k_1^\alpha I}{\sigma_1^\alpha\left(\alpha_1^\alpha+\alpha_2^\alpha+\delta_2^\alpha+\mu^\alpha\right)E_*}\\ &+ f(S_*, I_*)\left(\frac{\alpha_1^\alpha T_*}{\sigma_1^\alpha E_*} - \frac{\alpha_1^\alpha T}{\sigma_1^\alpha E_*} - \frac{\alpha_1^\alpha k_1^\alpha T_* I}{\sigma_1^\alpha\left(\alpha_1^\alpha+\alpha_2^\alpha+\delta_2^\alpha+\mu^\alpha\right)E_* T}\right).\end{aligned} \tag{3.9}$$

Adding Eqs (3.6)–(3.9), we have the following:

$$\begin{aligned}{}_0^cD_t^\alpha \Psi(t) \le\ & (\xi^\alpha + \mu^\alpha)\left(1-\frac{f(S_*, I_*)}{f(S, I_*)}\right)(S_* - S)\\ &+ f(S_*, I_*)\left(3 - \frac{f(S_*, I_*)}{f(S, I_*)} - \frac{f(S, I)E_*}{f(S_*, I_*)E} + \frac{f(S, I)}{f(S, I_*)} - \frac{I_*E}{IE_*} - \frac{I}{I_*}\right)\\ &+ g(S_*, E_*)\left(2 - \frac{f(S_*, I_*)}{f(S, I_*)} - \frac{g(S, E)E_*}{g(S_*, E_*)E} + \frac{f(S_*, I_*)g(S, E)}{f(S, I_*)g(S_*, E_*)} - \frac{E}{E_*}\right)\\ &+ f(S_*, I_*)\left(2\frac{\alpha_1^\alpha T_*}{\sigma_1^\alpha E_*} - \frac{\alpha_1^\alpha\left(\alpha_1^\alpha+\alpha_2^\alpha+\delta_2^\alpha+\mu^\alpha\right)T_*T}{\sigma_1^\alpha k_1^\alpha E_* I} - \frac{\alpha_1^\alpha k_1^\alpha T_* I}{\sigma_1^\alpha\left(\alpha_1^\alpha+\alpha_2^\alpha+\delta_2^\alpha+\mu^\alpha\right)E_* T}\right).\end{aligned}$$

After some calculations, we gain the following:

$$
\begin{aligned}
{}_0^cD_t^\alpha\Psi(t) \leq{}& (\xi^\alpha + \mu^\alpha)\left(1 - \frac{f(S_*, I_*)}{f(S, I_*)}\right)(S_* - S) \\
&+ f(S_*, I_*)\left(1 - \frac{f(S, I_*)}{f(S, I)}\right)\left(\frac{f(S, I)}{f(S, I_*)} - \frac{I}{I_*}\right) \\
&+ f(S_*, I_*)\left(4 - \frac{f(S_*, I_*)}{f(S, I_*)} - \frac{f(S, I_*)\, I}{f(S, I) I_*} - \frac{f(S, I) E_*}{f(S_*, I_*)\, E} - \frac{I_* E}{I E_*}\right) \\
&+ g(S_*, E_*)\left(1 - \frac{f(S, I_*)\, g(S_*, E_*)}{f(S_*, I_*)\, g(S, E)}\right)\left(\frac{f(S_*, I_*)\, g(S, E)}{f(S, I_*)\, g(S_*, E_*)} - \frac{E}{E_*}\right) \\
&+ g(S_*, E_*)\left(3 - \frac{f(S_*, I_*)}{f(S, I_*)} - \frac{f(S, I_*)\, g(S_*, E_*)\, E}{f(S_*, I_*)\, g(S, E) E_*} - \frac{g(S, E) E_*}{g(S_*, E_*)\, E}\right) \\
&+ f(S_*, I_*)\left(2\frac{\alpha_1^\alpha T_*}{\sigma_1^\alpha E_*} - \frac{\alpha_1^\alpha\left(\alpha_1^\alpha + \alpha_2^\alpha + \delta_2^\alpha + \mu^\alpha\right) T_* T}{\sigma_1^\alpha k_1^\alpha E_* I} - \frac{\alpha_1^\alpha k_1^\alpha T_* I}{\sigma_1^\alpha\left(\alpha_1^\alpha + \alpha_2^\alpha + \delta_2^\alpha + \mu^\alpha\right) E_* T}\right).
\end{aligned}
$$

Since $f(S, I)$ is a monotonically increasing function of S, we can see that

$$
\begin{aligned}
\frac{f(S_*, I_*)}{f(S, I_*)} &\geq 1, \forall S_* \geq S(t), \\
\frac{f(S_*, I_*)}{f(S, I_*)} &\leq 1, \forall S_* \leq S(t).
\end{aligned}
$$

Thus, $(S_* - S)\left(1 - \frac{f(S_*, I_*)}{f(S, I_*)}\right) \leq 0$. Using hypotheses (H_6) and (H_7), we find ${}_0^cD_t^\alpha\Psi(t) \leq 0$. By the LaSalle invariance principle, we conclude that the EEP P_* of the model (3.4) is GAS.

4. Numerical results and discussion

The spread of sex education has a direct impact on an individual's understanding of HIV and their awareness of preventive measures, which, in turn, influences their willingness and behaviors in adopting protective strategies. For susceptible individuals (S), sex education can increase their awareness of HIV risks and encourage behaviors such as consistent condom use and regular testing, which significantly reduce the likelihood of infection. Undiagnosed HIV-infected individuals (E), who unaware of their infection status, may unintentionally play a key role in transmitting the virus. For confirmed HIV-infected individuals (I), whether they take proactive preventive measures directly affects their risk of transmitting the virus.

In this section, we assume the infection forms are given by $g(S, E) = \frac{\beta_1 S E}{1+w_1 S+u_1 E}$ and $f(S, I) = \frac{\beta_2 S I}{1+w_2 S+u_2 I}$ to examine the effect of self-implemented preventive measures taken by three population groups—susceptible individuals, undiagnosed HIV-infected individuals, and confirmed HIV-infected individuals—on the spread of HIV. The specific model is as follows:

$$\begin{cases} {}_0^cD_t^\alpha S = \Lambda^\alpha - \frac{\beta_1 S E}{1+w_1 S+u_1 E} - \frac{\beta_2 S I}{1+w_2 S+u_2 I} - (\xi^\alpha + \mu^\alpha) S, \\ {}_0^cD_t^\alpha E = \frac{\beta_1 S E}{1+w_1 S+u_1 E} + \frac{\beta_2 S I}{1+w_2 S+u_2 I} - \left(\sigma_1^\alpha + \sigma_2^\alpha + \mu^\alpha\right) E, \\ {}_0^cD_t^\alpha I = \sigma_1^\alpha E + \alpha_1^\alpha T - \left(k_1^\alpha + k_2^\alpha + \mu^\alpha\right) I, \\ {}_0^cD_t^\alpha T = k_1^\alpha I - \left(\alpha_1^\alpha + \alpha_2^\alpha + \delta_2^\alpha + \mu^\alpha\right) T, \\ {}_0^cD_t^\alpha A = \sigma_2^\alpha E + k_2^\alpha I + \alpha_2^\alpha T - (\delta_1^\alpha + \mu^\alpha) A, \\ {}_0^cD_t^\alpha R = \xi^\alpha S - \mu^\alpha R, \end{cases} \tag{4.1}$$

with the non-negative initial conditions $S(0) = S^0, E(0) = E^0, I(0) = I^0, T(0) = T^0, A(0) = A^0$, and $R(0) = R^0$. Here, u_1 and u_2 represent the levels of preventive measures adopted by undiagnosed and confirmed HIV-infected individuals, respectively, during sexual contact with susceptible individuals. On the other hand, w_1 and w_2 indicate the levels of protective measures taken by susceptible individuals when in contact with these two groups of infected individuals, respectively.

Now, we verify that $g(S, E) = \frac{\beta_1 S E}{1+w_1 S+u_1 E}$ and $f(S, I) = \frac{\beta_2 S I}{1+w_2 S+u_2 I}$ satisfy the hypotheses $(H1) \sim (H6)$. Obviously, hypotheses $(H1) \sim (H2)$ are satisfied.

Since $0 < \frac{\partial g(S,E)}{\partial S} \leqslant \frac{\beta_1}{u_1}$ and $0 < \frac{\partial f(S,I)}{\partial S} \leqslant \frac{\beta_2}{u_2}$, hypothesis $(H3)$ holds.

Since $0 < \frac{\partial g(S,E)}{\partial E} = \frac{\beta_1 S + w_1\beta_1 S^2}{(1+w_1 S+u_1 E)^2} \leqslant \frac{g(S,E)}{E}$ and $0 < \frac{\partial f(S,I)}{\partial I} = \frac{\beta_2 S + w_2\beta_2 S^2}{(1+w_2 S+u_2 I)^2} \leqslant \frac{f(S,I)}{I}$, hypothesis $(H4)$ holds.

Since $\frac{\partial^2 g(S,E)}{\partial E^2} = \frac{-2u_1(\beta_1 S + w_1\beta_1 S^2)}{(1+w_1 S+u_1 E)^3} \leqslant 0$ and $\frac{\partial^2 f(S,I)}{\partial I^2} = \frac{-2u_2(\beta_2 S + w_2\beta_2 S^2)}{(1+w_2 S+u_2 I)^3} \leqslant 0$, hypothesis $(H5)$ holds.

Since $\left(1 - \frac{f(S,I_*)}{f(S,I)}\right)\left(\frac{f(S,I)}{f(S,I_*)} - \frac{I}{I_*}\right) = \frac{-u_2(1+w_2 S)(I-I_*)^2}{(1+w_2 S+u_2 I)(1+w_2 S+u_1 I_*)I_*} \leqslant 0$, it is obvious that hypothesis $(H6)$ holds. For condition $(H7)$, we discuss the following three cases:

Case1. When $w_1 = w_2 = u_1 = u_2 = 0$, $g(S, E) = \beta_1 S E$, $f(S, I) = \beta_2 S I$, then we have $\left(1 - \frac{f(S,I_*)g(S_*,E_*)}{f(S_*,I_*)g(S,E)}\right)\left(\frac{f(S_*,I_*)g(S,E)}{f(S,I_*)g(S_*,E_*)} - \frac{E}{E_*}\right) = 0$, which satisfies hypothesis $(H7)$.

Case2. When $w_1 = w_2 = u_1 = 0$, $g(S, E) = \beta_1 S E$, $f(S, I) = \frac{\beta_2 S I}{1+u_2 I}$, then we have $\left(1 - \frac{f(S,I_*)g(S_*,E_*)}{f(S_*,I_*)g(S,E)}\right)\left(\frac{f(S_*,I_*)g(S,E)}{f(S,I_*)g(S_*,E_*)} - \frac{E}{E_*}\right) = 0$, which satisfies hypothesis $(H7)$.

Case3. When $w_1 = w_2 = 0$, $g(S, E) = \frac{\beta_1 S E}{1+u_1 E}$, $f(S, I) = \frac{\beta_2 S I}{1+u_2 I}$, then we have $\left(1 - \frac{f(S,I_*)g(S_*,E_*)}{f(S_*,I_*)g(S,E)}\right)\left(\frac{f(S_*,I_*)g(S,E)}{f(S,I_*)g(S_*,E_*)} - \frac{E}{E_*}\right) = \frac{-u_1(E-E_*)^2}{E_*(1+u_1 E)(1+u_1 E_*)}$, which satisfies hypothesis $(H7)$.

The basic reproduction number of model (4.1) is $R_0^\alpha = R_E^\alpha + R_I^\alpha$, where $R_E^\alpha = \frac{\beta_1\Lambda^\alpha}{(\sigma_1^\alpha+\sigma_2^\alpha+\mu^\alpha)(\xi^\alpha+\mu^\alpha+w_1\Lambda^\alpha)}$, and $R_I^\alpha = \frac{\beta_2\Lambda^\alpha D}{C(\sigma_1^\alpha+\sigma_2^\alpha+\mu^\alpha)(\xi^\alpha+\mu^\alpha+w_2\Lambda^\alpha)}$.

4.1. Numerical scheme for the solution

In the field of numerical computation for fractional-order differential equations, there are finite difference methods such as explicit schemes, implicit schemes, the Crank–Nicholson method, predictor–corrector methods, and integral equation methods, as well as certain finite element methods, meshless methods, and matrix methods (for example, see [6, 17, 18] and the references therein). Now, we discuss the numerical format of the solution of model (4.1) with the idea of an Adams-Bashforth-Moulton predictive correction, and consider the following fractional differential equation [6]:

$${}_0^cD_t^\alpha \Phi(t) = g(t, \Phi(t)), \quad 0 \le t \le \tau,$$

with the initial conditions

$$\Phi^k(0) = \Phi_0^k, \quad k = 0, 1, 2, \dots, \lceil\alpha\rceil - 1.$$

Its corresponding fractional integral equation is as follows:

$$\Phi(t) = \sum_{k=0}^{\lceil\alpha\rceil-1} \frac{\Phi_0^{(k)}}{k!} t^k + \frac{1}{\Gamma(\alpha)} \int_0^t (t-x)^{\alpha-1} g(x, \Phi(x)) dx.$$

Take the step h, node $t = nh$, $n = 0, 1, 2, \ldots, N$ on the integral interval $[0, t]$, and then, approximate by the trapezoidal integral formula to get the following:

$$\begin{aligned}\Phi_h(t_{n+1}) = {} & \sum_{k=0}^{\lceil\alpha\rceil-1} \frac{\Phi_0^{(k)}}{k!} t_{n+1}^k + \frac{h^\alpha}{\Gamma(\alpha+2)} g\left(t_{n+1}, \Phi_h^P(t_{n+1})\right) \\ & + \frac{h^\alpha}{\Gamma(\alpha+2)} \sum_{q=0}^{n} c_{q,n+1} g\left(t_q, \Phi_h\left(t_q\right)\right),\end{aligned}$$

where

$$c_{q.n+1} = \begin{cases} n^{\alpha+1} - (n-\alpha)(n+\alpha)^\alpha; \quad q = 0 \\ (n-q+2)^{\alpha+1} + (n-q)^{\alpha+1} - 2(n-q+1)^{\alpha+1}; \quad 0 < q \le n \\ 1; \quad q = n+1. \end{cases}$$

And the predicted value $\Phi_h^P(t_{n+1})$ is evaluated by the following:

$$\Phi_h^P(t_{n+1}) = \sum_{k=0}^{\lceil\alpha\rceil-1} \frac{\Phi_0^{(k)}}{k!} t_{n+1}^k + \frac{1}{\Gamma(\alpha)} \sum_{q=0}^{n} d_{q,n+1} g\left(t_q, \Phi_h\left(t_q\right)\right)$$

with

$$d_{q,n+1} = \frac{h^\alpha}{\alpha}\left((n+1-q)^\alpha - (n-q)^\alpha\right).$$

The error estimate is given by the following expression:

$$\max_{q=0,1,2,\ldots,N} \left|\Phi\left(t_q\right) - \Phi_h\left(t_q\right)\right| = O\left(h^p\right),$$

where $p = \min(2, 1+\alpha)$.

In the computation of the numerical solution, the step size $h = 0.01$ is used throughout the numerical simulations.

4.2. Stability analysis of DFE

This section examines the stability of the DFE across various initial conditions. The following parameter values are chosen for the model (4.1) to ensure $R_0^\alpha = 0.8635 < 1$: $\alpha = 0.998, \Lambda = 0.015, \beta_1 = 0.22, \beta_2 = 0.18, u_1 = 0.5, u_2 = 0.6, w_1 = 0.21, w_2 = 0.32, \xi = 0.001, \sigma_1 = 0.45, \sigma_2 = 0.1, k_1 = 0.34, k_2 = 0.1, \alpha_1 = 0.32, \alpha_2 = 0.08, \mu = 0.01416, \delta_1 = 0.01464$, and $\delta_2 = 0.01034$. The various starting conditions are listed as in Table 2.

Table 2. The starting conditions for the model (4.1).

Case	$S(0)$	$E(0)$	$I(0)$	$T(0)$	$A(0)$	$R(0)$
1	0.9	0.02	0.025	0.01	0.003	0.042
2	0.8	0.04	0.045	0.015	0.006	0.094
3	0.7	0.06	0.065	0.025	0.01	0.14
4	0.6	0.08	0.085	0.045	0.02	0.17
5	0.5	0.1	0.1	0.065	0.045	0.19
6	0.4	0.12	0.125	0.085	0.06	0.21
7	0.3	0.14	0.15	0.1	0.08	0.23

Figure 1 displays the changes in the proportions of $S, E + I + T + A$, and R over time. Figure 1(a) shows the time evolution of the proportion of susceptible individuals S. Figure 1(b) illustrates the time variation of the combined group $E + I + T + A$, and Figure 1(c) depicts the change in the proportion of low-risk individuals R over time. The image reveals that all the curves in Figure 1(a) eventually converge to the value $\frac{\Lambda^\alpha}{\xi^\alpha+\mu^\alpha}$. In Figure 1(b), the proportions of E, I, T, and A decrease over time and approach 0. The curves in Figure 1(c) stabilize at $\frac{\xi^\alpha\Lambda^\alpha}{\mu^\alpha(\xi^\alpha+\mu^\alpha)}$ as time progresses. This not only demonstrates the stability of the DFE but also shows that the system's stability is independent of the initial conditions, with all variables ultimately converging to the DFE $P_0 = \left(\frac{\Lambda^\alpha}{\xi^\alpha+\mu^\alpha}, 0, 0, 0, 0, \frac{\xi^\alpha\Lambda^\alpha}{\mu^\alpha(\xi^\alpha+\mu^\alpha)}\right)$.

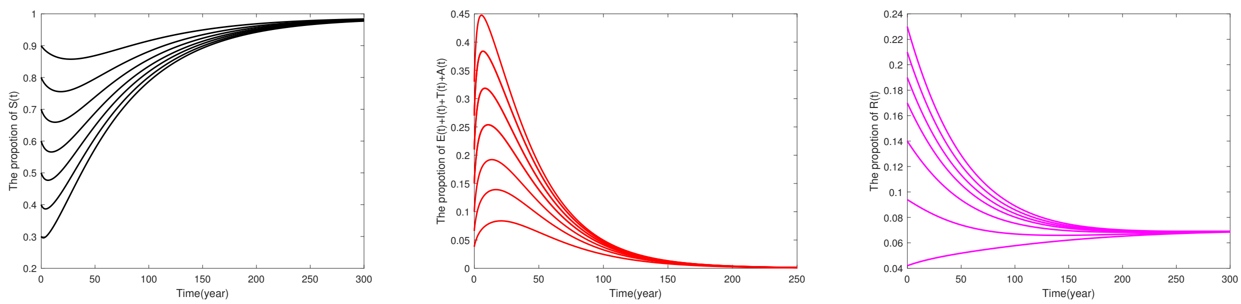

(a) Variation of S over time.

(b) Variation of $E+I+T+A$ over time.

(c) Variation of R over time.

Figure 1. Variation of the propotion of $S, E+I+T+A$, and R over time with different initial values, $R_0^\alpha = 0.8635 < 1$.

4.3. Stability analysis of EEP

This section examines the stability of the EEP under the condition $R_0^\alpha = 1.8582 > 1$. The parameter values used in the model (4.1) are specified as follows: $\alpha = 0.998, \Lambda = 0.015, \beta_1 = 0.38, \beta_2 = 0.30, \xi = 0.001, \sigma_1 = 0.45, \sigma_2 = 0.1, k_1 = 0.34, k_2 = 0.1, \alpha_1 = 0.32, \alpha_2 = 0.08, \mu = 0.01416, \delta_1 = 0.01464$, and $\delta_2 = 0.01034$. The various starting conditions are shown in Table 2. The stability characteristics of the EEP under three different scenarios are shown in Figures 2–4. The results indicate that the system's stability demonstrates global convergence, meaning that the system's behavior is independent of the initial conditions and, in all cases, it ultimately converges to the EEP.

Case1. When $w_1 = w_2 = u_1 = u_2 = 0$, $g(S, E) = \beta_1 SE$, $f(S, I) = \beta_2 SI$.

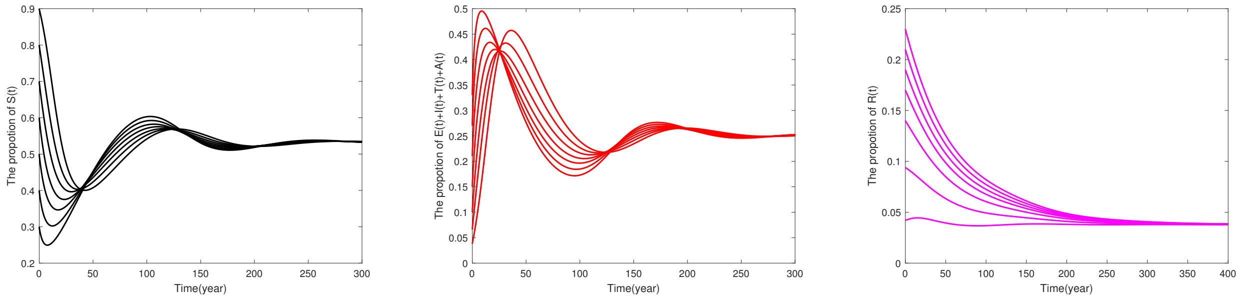

(a) Variation of S over time.

(b) Variation of $E+I+T+A$ over time.

(c) Variation of R over time.

Figure 2. Variation of the propotion of S, $E+I+T+A$, and R over time with different initial values.

Case2. When $w_1 = w_2 = u_1 = 0$ and $u_2 = 0.6$, $g(S,E) = \beta_1 SE$, $f(S,I) = \frac{\beta_2 SI}{1+u_2 I}$.

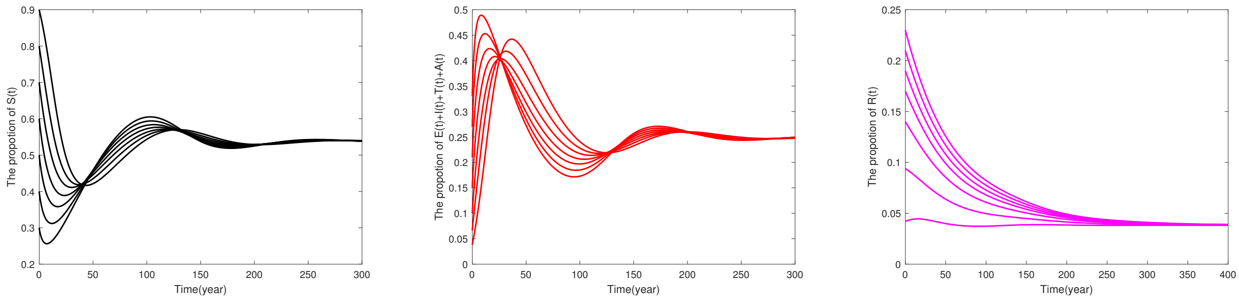

(a) Variation of S over time.

(b) Variation of $E+I+T+A$ over time.

(c) Variation of R over time.

Figure 3. Variation of the propotion of S, $E+I+T+A$, and R over time with different initial values.

Case3. When $w_1 = w_2 = 0$, $u_1 = 0.5$, and $u_2 = 0.6$, $g(S,E) = \frac{\beta_1 SE}{1+u_1 E}$, $f(S,I) = \frac{\beta_2 SI}{1+u_2 I}$.

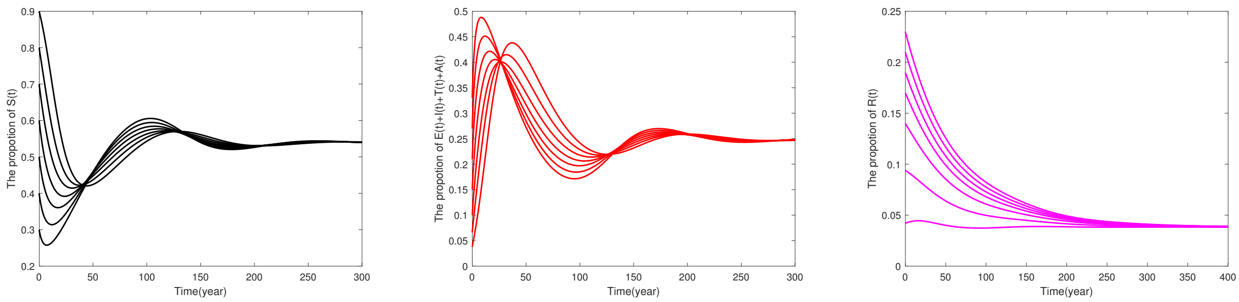

(a) Variation of S over time.

(b) Variation of $E+I+A+T$ over time.

(c) Variation of R over time.

Figure 4. Variation of the propotion of S, $E+I+T+A$, and R over time with different initial values.

4.4. Experimental analysis

In this section, we conduct a series of experimental investigations utilizing actual HIV data from Mexico covering the period from 1990 to 2019. The study aims to forecast the trajectory of the HIV epidemic in Mexico, with a specific emphasis on evaluating how the extent of preventive actions taken by susceptible individuals (S) during interactions with undiagnosed HIV-infected individuals (E) and confirmed HIV-infected individuals (I) influences disease transmission. The goal is to assess the extent to which these measures can curb the spread of the disease. According to historical records from [38], by the end of 1990, Mexico's approximate total population was 83,943,132, and the cumulative number of reported HIV cases reached 37,519. Based on this, we assume the initial conditions to be as follows: $S(0) = 83,885,626, E(0) = 20000, I(0) = 25000, T(0) = 10000, A(0) = 2519$, and $R(0) = 0$. We employ the fminsearch routine in MATLAB to refine the fitting of the remaining parameters such that the approximate solution of model (4.1) aligns more closely with real-world data. This method utilizes the Nelder-Mead simplex algorithm to minimize the discrepancy between the model output and the observed data. Figure 5 presents the specific simulation results of model (4.1). Table 3 provides the specific assigned values for all key parameters in model (4.1).

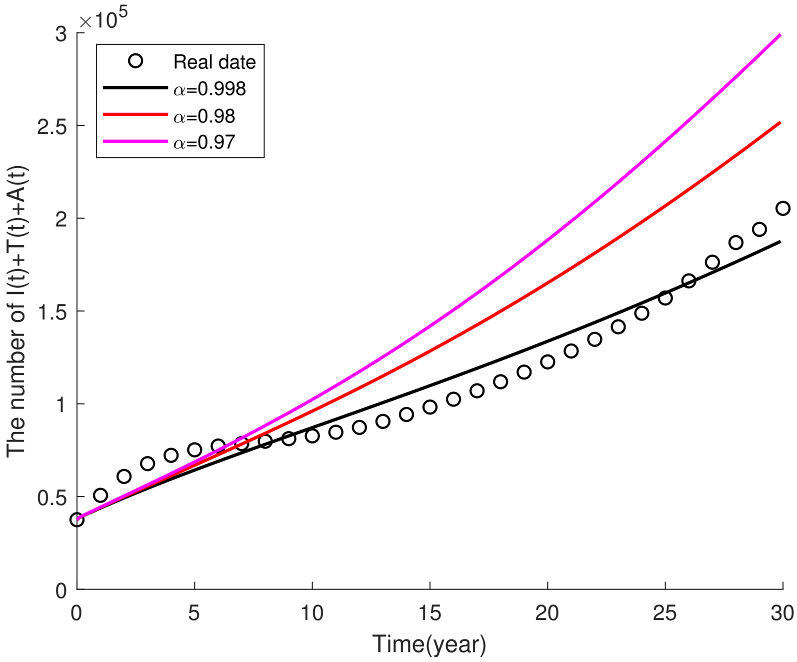

Figure 5. The comparison between simulated data and real data for the model (4.1).

Table 3. Prediction values of the model (4.1).

Parameter	Value	Sources	Parameter	Value	Sources
Λ	1188634	[6]	ξ	0.01	Fitted
β_1	0.562×10^{-3}	Fitted	β_2	0.153×10^{-3}	Fitted
u_1	0.5	Fitted	u_2	0.6	Fitted
w_1	0.0021	Fitted	w_2	0.0032	Fitted
σ_1	0.32	Fitted	σ_2	0.009	Fitted
k_1	0.34	Fitted	k_2	0.01	Fitted
α_1	0.32	Fitted	α_2	0.008	Fitted
μ	0.01416	[6]	δ_1	0.01464	Assumed
δ_2	0.01034	Assumed			

4.4.1. Model comparison

To further assess the efficacy of the proposed model, this study performed a comparative analysis against the models introduced by Huo et al. and S. Mangal et al. The model proposed by Huo et al. [4]. overlooked the influence of undiagnosed HIV-infected individuals on the spread of HIV, and its transmission dynamics were characterized by the incidence rate βSI. The differential equations for this model can be written as follows:

$$\begin{cases} \dot{S} = \Lambda - \beta IS - \mu_1 S - dS, \\ \dot{I} = \beta IS + \alpha_1 T - dI - k_1 I - k_2 I, \\ \dot{A} = k_1 I - (\delta_1 + d)A + \alpha_2 T, \\ \dot{T} = k_2 I - \alpha_1 T - (d + \delta_2 + \alpha_2)T, \\ \dot{R} = 1S - dR. \end{cases} \tag{4.2}$$

In comparison, the model developed by S. Mangal et al. [6] incorporated a state variable E to denote individuals infected with HIV who were not yet diagnosed. The incidence rate in this framework is composed of two components: $(1 - w)\beta SE$ and $\frac{\beta SI}{1+uI}$. While this model accounted for the influence of preventive actions by both undiagnosed and confirmed HIV-positive individuals on HIV transmission, it did not adequately capture the critical aspect of susceptible individuals who also adopted preventive measures when interacting with those infected. The fractional-order equations which represent this transmission model can be formulated as follows:

$$\begin{cases} {}_0^cD_t^\alpha S = \Pi^\alpha - (1 - w)\beta_1^\alpha SE - \dfrac{\beta_2^\alpha SI}{1 + uI} - (\xi + \mu^\alpha)S, \\ {}_0^cD_t^\alpha E = (1 - w)\beta_1^\alpha SE + \dfrac{\beta_2^\alpha SI}{1 + uI} - (\sigma_1^\alpha + \sigma_2^\alpha + \mu^\alpha)E, \\ {}_0^cD_t^\alpha I = \sigma_1^\alpha E + \alpha_1^\alpha T - (k_1^\alpha + k_2^\alpha + \mu^\alpha)I, \\ {}_0^cD_t^\alpha T = k_2^\alpha I - (\alpha_1^\alpha + \alpha_2^\alpha + \delta_2^\alpha + \mu^\alpha)T, \\ {}_0^cD_t^\alpha A = \sigma_2^\alpha E + k_1^\alpha I + \alpha_2^\alpha T - (\delta_1^\alpha + \mu^\alpha)A, \\ {}_0^cD_t^\alpha R = \xi S - \mu^\alpha R. \end{cases} \tag{4.3}$$

Figure 6 presents the specific simulation results of model (4.2). The parameter values for model (4.2) are presented in Table 4, while the specific simulation results and the parameter details for model (4.3) are available in reference [6].

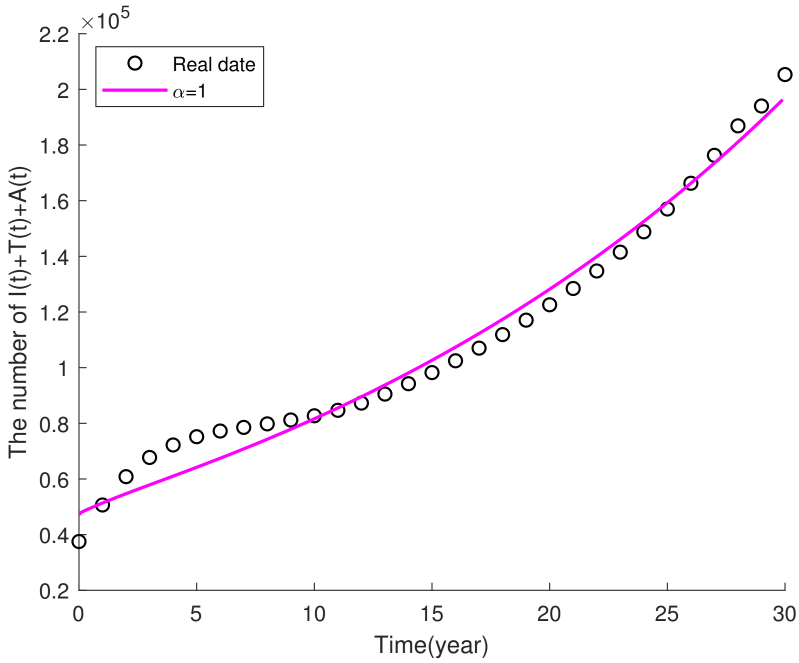

Figure 6. The comparison between simulated data and real data for the model (4.2).

Remark 4.1. Model (3.1) degenerates to model (4.3) when $f(S, I) = (1 - w)\beta_1^{\alpha} S E$ and $g(S, E) = \frac{\beta_2^{\alpha} S I}{1+uI}$.

Table 4. Prediction values of the model (4.2).

Parameter	Value	Sources	Parameter	Value	Sources
Λ	1188634	[6]	u_1	0.001	Fitted
β	0.158×10^{-8}	Fitted	d	0.01416	[6]
k_2	0.34	Fitted	k_1	0.01	Fitted
α_1	0.32	Fitted	α_2	0.008	Fitted
δ_1	0.01464	Assumed	δ_2	0.01034	Assumed

As illustrated in Figure 7, a comparison of the three models reveals that, in terms of the number of HIV-infected individuals, the predicted population size of both undiagnosed and confirmed HIV-infected individuals in model (4.1) do not escalate to an unmanageable level. This aligns with real-world scenarios where prevention and control measures proved to be effective. Additionally, the numbers of HIV patients undergoing treatment and those with full-blown AIDS are more realistic, thus reflecting a balance between the allocation of medical resources and the willingness of patients to accept treatment. In contrast to the other two models, model (4.1) provides a more accurate representation of HIV epidemic trends and the effects of prevention and control measures.

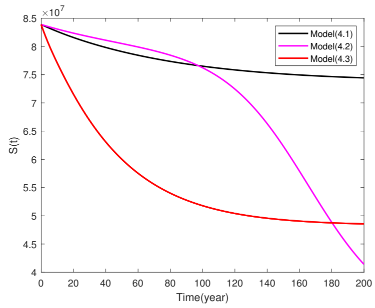

(a) Variation of S over time.

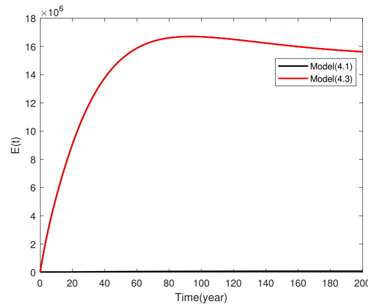

(b) Variation of E over time.

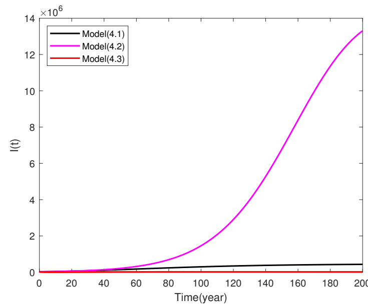

(c) Variation of I over time.

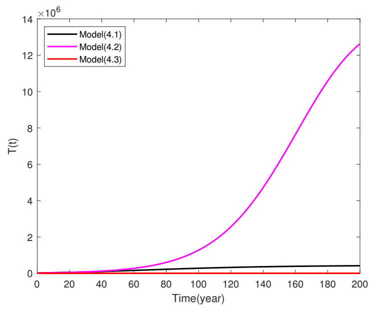

(d) Variation of T over time.

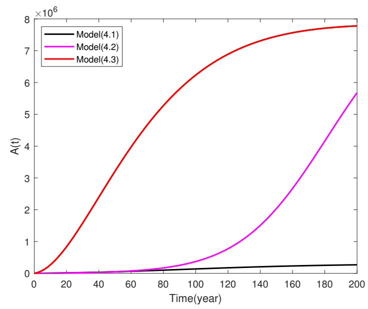

(e) Variation of A over time.

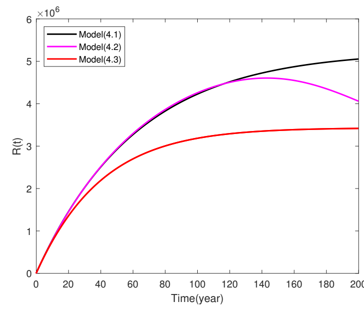

(f) Variation of R over time.

Figure 7. Variation of the number of S, E, I, T, A, and R over time in different models.

4.4.2. Sensitivity analysis of R_0^α, R_E^α and R_I^α

The basic reproduction number serves as a vital indicator to evaluate the transmission potential of a disease, where higher values signify a greater risk of spread. In this section, we focus on analyzing the influence of key parameters w_1 (represents the level of preventive measures during interactions between susceptible individuals and undiagnosed HIV-infected individuals) and w_2 (represents the level of preventive measures during interactions between susceptible individuals and confirmed HIV-infected individuals) on the basic reproduction numbers R_E^α and R_I^α. As shown in Figure 8, the basic reproduction number R_E^α for undiagnosed HIV-infected individuals significantly decreases as w_1 increases, whereas R_I^α for confirmed HIV-infected individuals remains unchanged by variations in w_1. Conversely, R_I^α decreases with an increase in w_2, while R_E^α is unaffected by changes in w_2. These findings highlight that increasing w_1 and w_2 can effectively lower R_0^α, thereby reducing the spread of the disease.

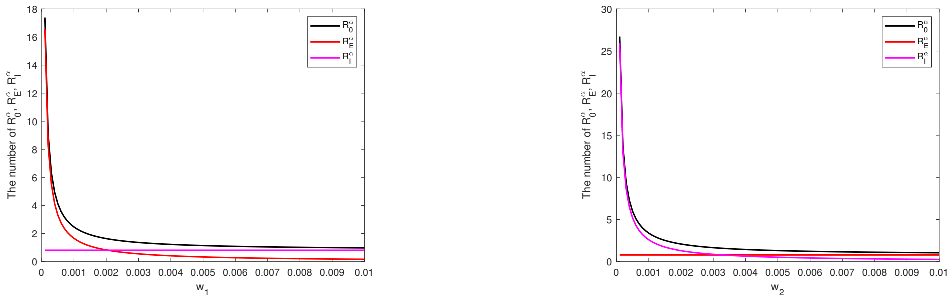

(a) Variation of R_0^α, R_E^α, R_I^α with w_1

(b) Variation of R_0^α, R_E^α, R_I^α with w_2.

Figure 8. Variation of R_0^α, R_E^α, R_I^α varying with w_1 and w_2, respectively.

4.4.3. Forecasting the future trend and control of HIV/AIDS in Mexico

Figure 9 demonstrates the dynamic evolution trends of various population groups under different fractional-order α values, thereby encompassing susceptible individuals, undiagnosed HIV-infected individuals, confirmed HIV-infected individuals, individuals receiving treatment, full-blown AIDS patients, and low-risk individuals. These insights clarify the projected trajectory of HIV/AIDS transmission dynamics in Mexico.

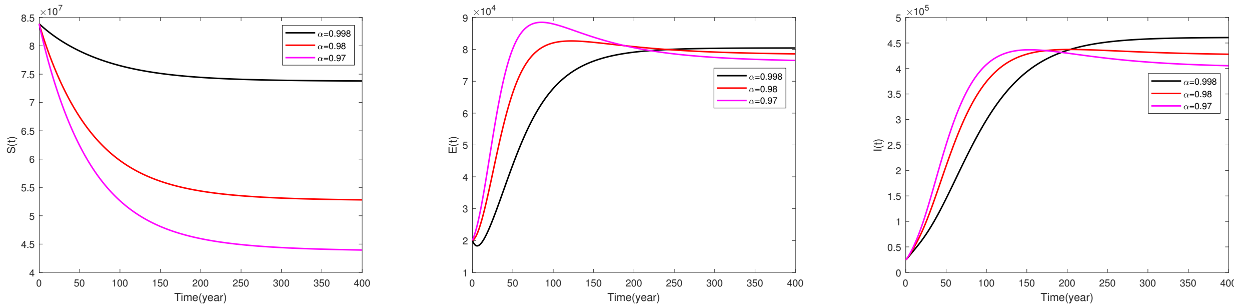

(a) Variation of S over time.

(b) Variation of E over time.

(c) Variation of I over time.

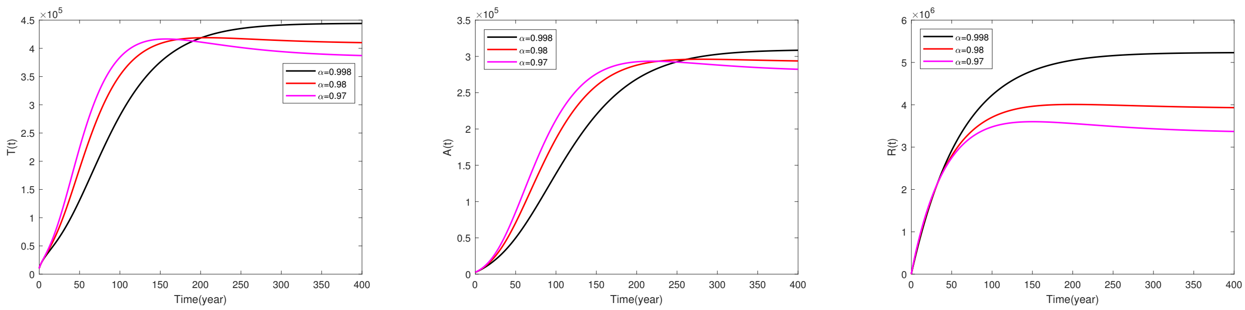

(d) Variation of T over time.

(e) Variation of A over time.

(f) Variation of R over time.

Figure 9. Forecasting of the future disease dynamics in the context of Mexico with R_0^α = 1.6001, 1.7615, and 1.8581 for α = 0.998, 0.98, and 0.97, respectively.

As shown in Figures 10–12, the research findings highlight the influence of the level of preventive measures adopted by HIV-infected individuals on the transmission of the disease. Figure 10(a)–(d) reveal that as the implementation level of preventive measures among undiagnosed HIV-infected individuals (u_1) increases, the scale of the epidemic across various infection categories shows a declining trend. Similarly, Figure 11(a)–(d) indicate that enhancing the implementation level of preventive measures among confirmed HIV-infected individuals (u_2) results in a significant reduction in the epidemic scale across all infection categories. Figure 12(a)–(d) further demonstrate that simultaneously increasing the values of u_1 and u_2 leads to a more pronounced decline in the epidemic scale of all infection categories compared to individually enhancing either u_1 or u_2. This finding suggests that dual preventive measures which target both undiagnosed and confirmed HIV-infected individuals have a synergistic effect, thus producing a more substantial impact on disease control. However, since the basic reproduction number R_0^α is independent of u_1 and u_2, and although raising u_1 and u_2 can effectively reduce disease transmission, it does not achieve the complete eradication of the disease.

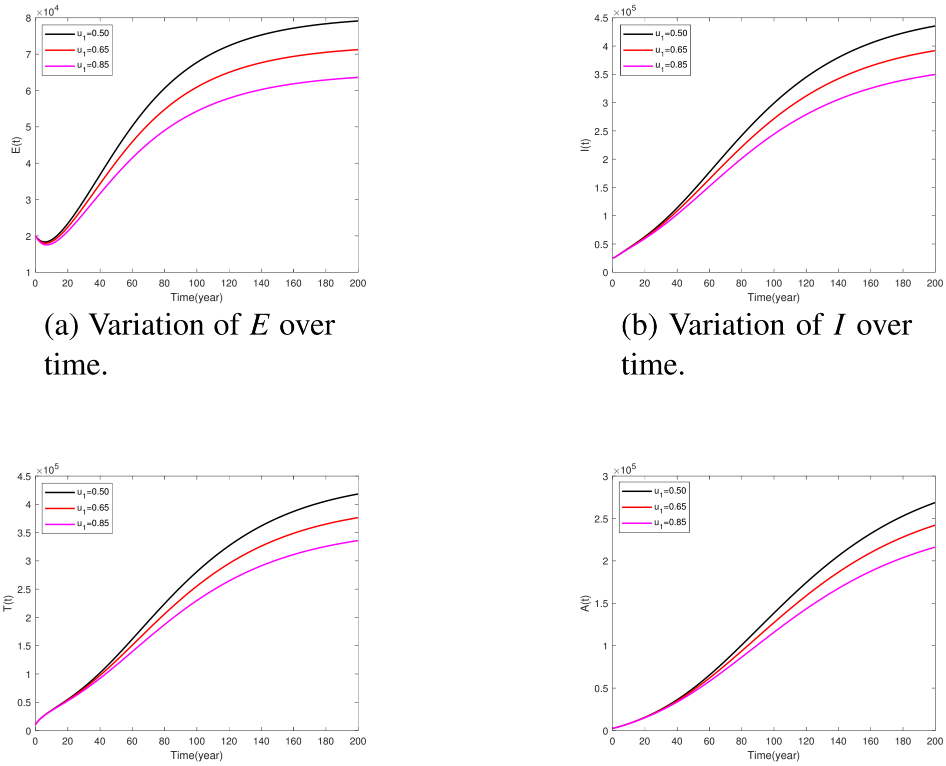

(a) Variation of E over time.

(b) Variation of I over time.

(c) Variation of T over time.

(d) Variation of A over time.

Figure 10. Forecasting of the disease in the context of Mexico when u_1 changes, R_0^α = 1.6001, R_E^α = 0.7895, and R_I^α = 0.8106, respectively.

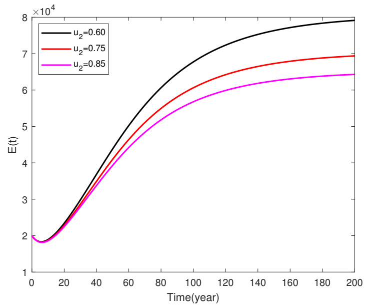

(a) Variation of E over time.

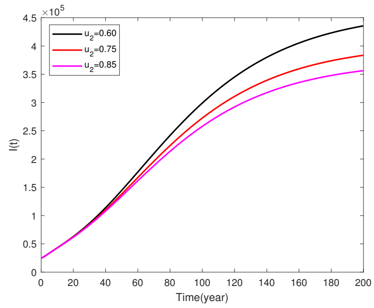

(b) Variation of I over time.

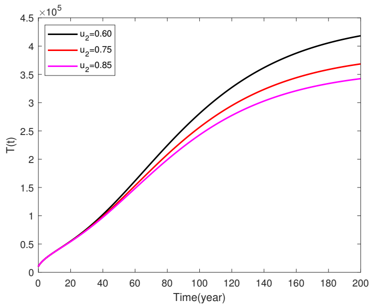

(c) Variation of T over time.

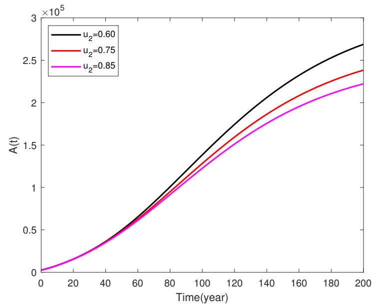

(d) Variation of A over time.

Figure 11. Forecasting of the disease in the context of Mexico when u_2 changes, $R_0^\alpha = 1.6001$, $R_E^\alpha = 0.7895$, and $R_I^\alpha = 0.8106$, respectively.

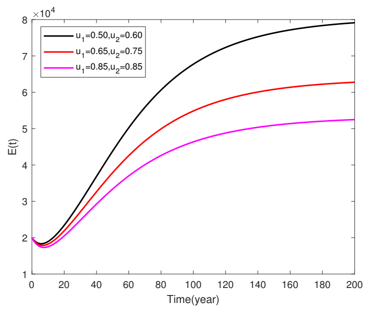

(a) Variation of E over time.

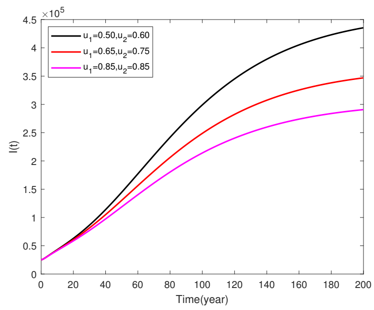

(b) Variation of I over time.

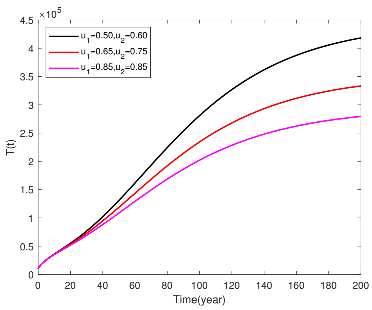

(c) Variation of T over time.

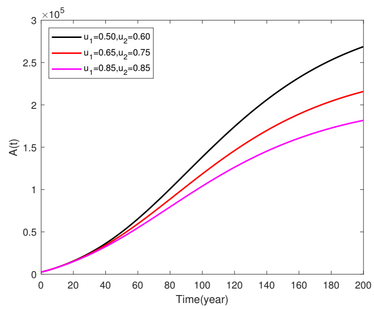

(d) Variation of A over time.

Figure 12. Forecasting of the disease in the context of Mexico for various values of u_1 and u_2, $R_0^\alpha = 1.6001$, $R_E^\alpha = 0.7895$, and $R_I^\alpha = 0.8106$, respectively.

As depicted in Figures 13–15, the level of protective measures adopted by susceptible individuals during interactions with HIV-infected individuals can effectively reduce the spread of the disease. Figure 13(a)–(d) show that as the level of preventive measures (w_1) taken by susceptible individuals during contact with undiagnosed HIV-infected individuals increases, the prevalence scale of each infection category exhibits a significant decline.

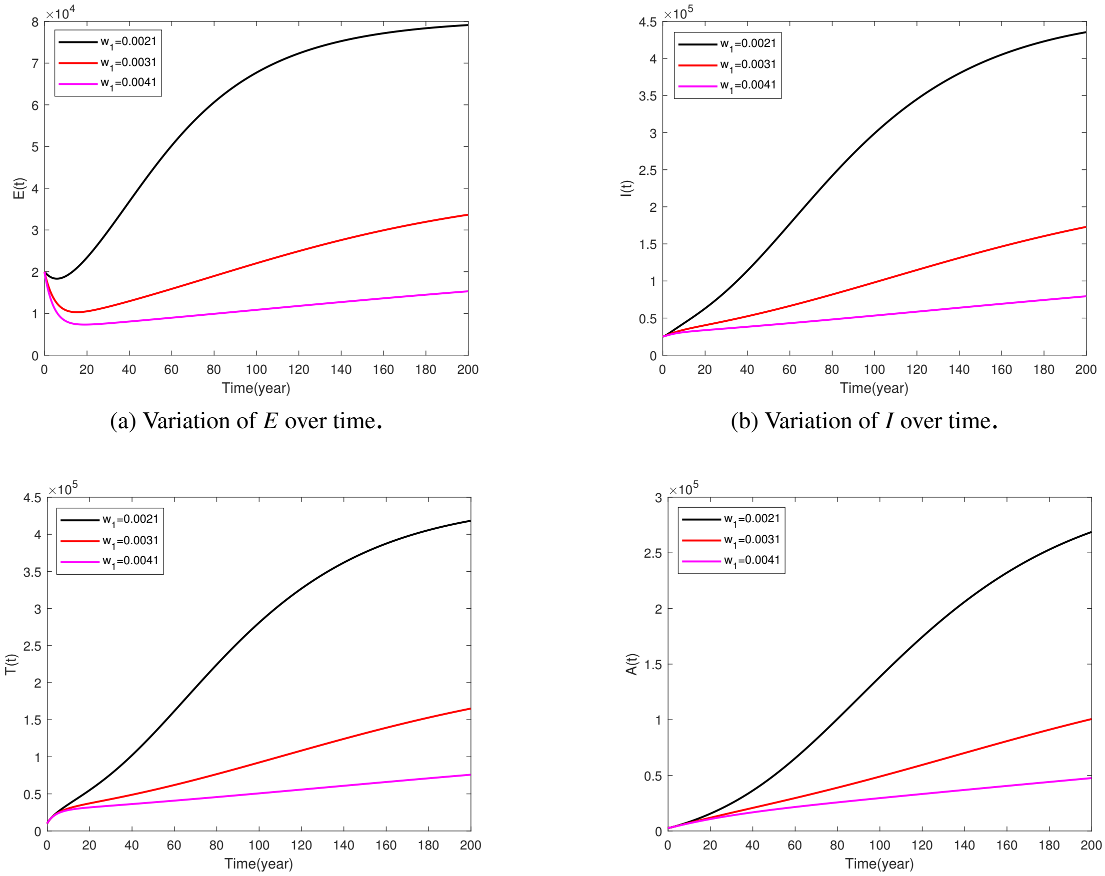

(a) Variation of E over time. (b) Variation of I over time.

(c) Variation of T over time. (d) Variation of A over time.

Figure 13. Forecasting of the disease in the context of Mexico for various values of w_1 and $(R_0^\alpha, R_E^\alpha, R_I^\alpha)$=(1.6001,0.7895,0.8106), (1.3454,0.5348,0.8106), (1.2150,0.4044,0.8106) corresponding to w_1=0.0021, 0.0031, and 0.0041, respectively.

Additionally, Figure 14(a)–(d) illustrate that strengtheningthe levelofpreventivemeasures (w2) implementedbysusceptible individualsduring contactwithconfirmedHIV-infected individuals effectively reduces theprevalence scaleof each infectioncategory.

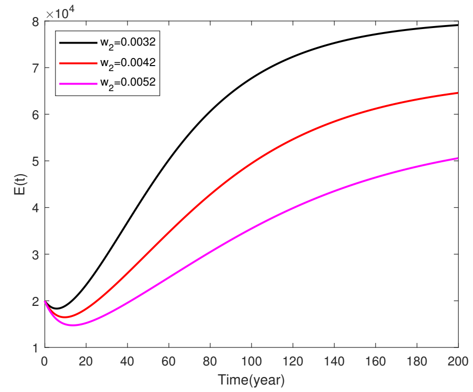

(a) Variation of E over time.

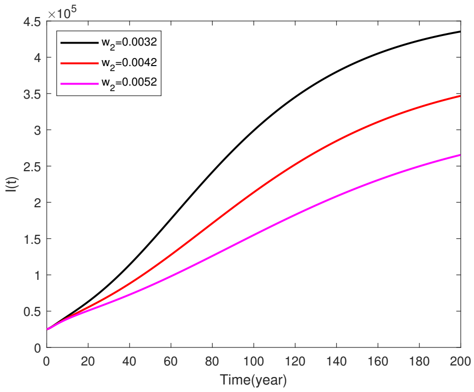

(b) Variation of I over time.

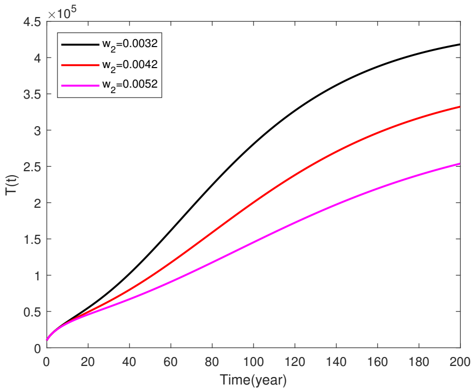

(c) Variation of T over time.

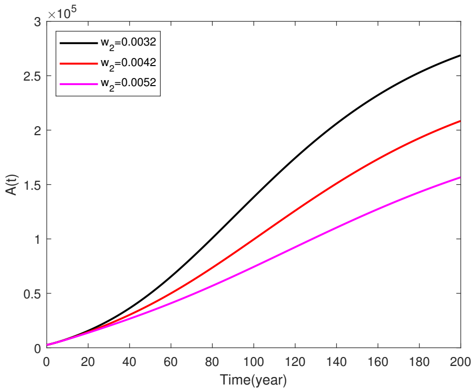

(d) Variation of A over time.

Figure 14. Forecasting of the disease in the context of Mexico for various values of w_2 and $(R_0^\alpha, R_E^\alpha, R_I^\alpha)$=(1.6001,0.7895,0.8106), (1.4071,0.7895,0.6176), (1.2883,0.7895,0.4988) corresponding to w_1=0.0021, 0.0031, and 0.0041, respectively.

Moreover, Figure 15(a)–(b) reveal that simultaneously increasing the values of w_1 and w_2 leads to a more pronounced reduction in the prevalence scale of each infection category compared to individually. It is important to note that w_1 and w_2 are key control parameters, with w_1 significantly impacting the basic reproduction number R_E^α of undiagnosed HIV-infected individuals, and w_2 significantly affecting the basic reproduction number R_I^α of confirmed HIV-infected individuals. By synergistically increasing w_1 and w_2, the basic reproduction number R_0^α can be minimized to the greatest extent.

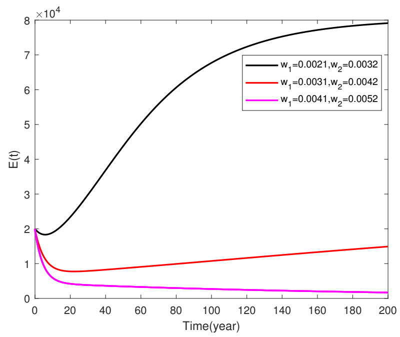

(a) Variation of E over time.

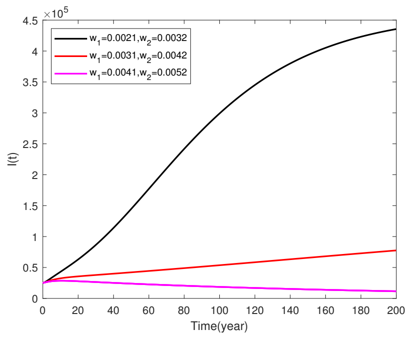

(b) Variation of I over time.

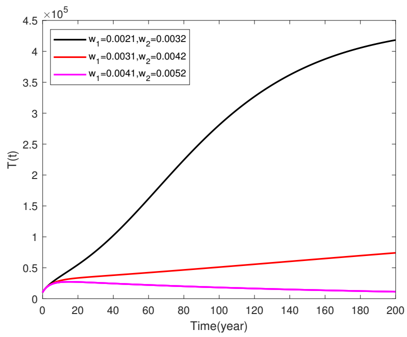

(c) Variation of T over time.

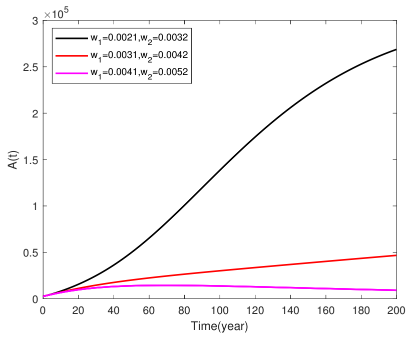

(d) Variation of A over time.

Figure 15. Forecasting of the disease in the context of Mexico for various values of control measures with $(R_0^\alpha, R_E^\alpha, R_I^\alpha)$=(1.6001,0.7895,0.8106), (1.1524,0.5348,0.6176), (0.9032,0.4044,0.4988) corresponding to (w_1, w_2)=(0.0021, 0.0032), (0.0031,0.0042) and (0.0041,0.0052), respectively.

As depicted in Figure 16, when u_1, u_2, w_1, and w_2 increase, the infected population experience a rapid and significant decline, thus requiring less time to be eradicated. Therefore, u_1, u_2, w_1, and w_2 can be considered the most effective control strategies to curb the spread of HIV/AIDS and shorten the time required for its elimination.

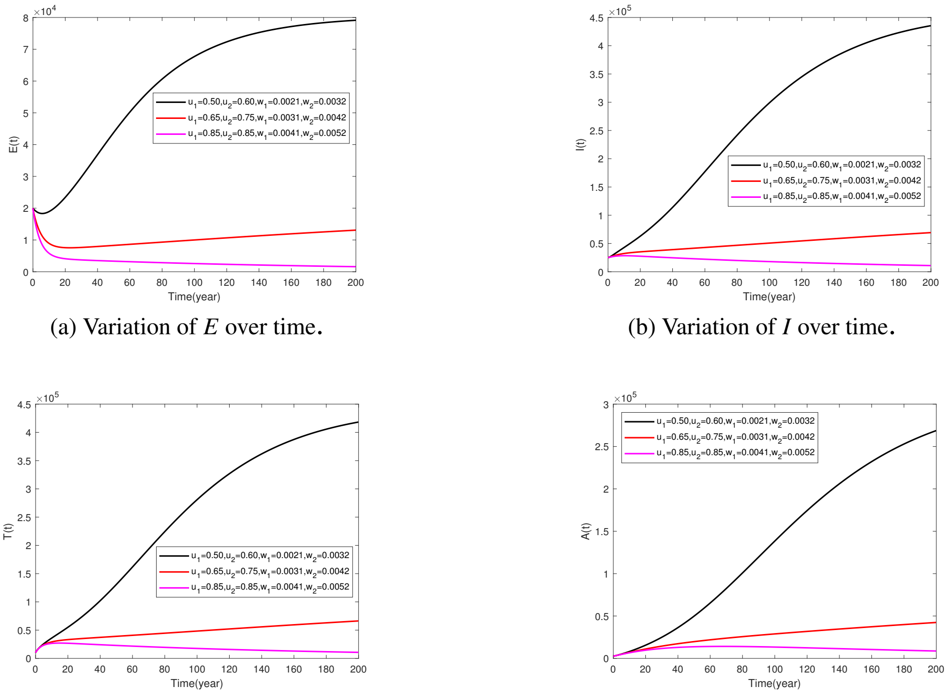

(a) Variation of E over time.

(b) Variation of I over time.

(c) Variation of T over time.

(d) Variation of A over time.

Figure 16. Forecasting of the disease in the context of Mexico for various values of control measures with $(R_0^\alpha, R_E^\alpha, R_I^\alpha)$=(1.6001,0.7895,0.8106), (1.1524,0.5348,0.6176), (0.9032,0.4044,0.4988) corresponding to (u_1, u_2, w_1, w_2)=(0.50,0.60,0.0021,0.0032), (0.65,0.75,0.0031,0.0042), and (0.85,0.85,0.0041,0.0052), respectively.

5. Conclusions

This paper examined a fractional-order HIV/AIDS model that incorporated nonlinear incidence rates represented by $f(S, I)$ and $g(S, E)$. To guarantee the model's validity and applicability, we introduced a set of mathematical assumptions, denoted as $(H_1) \sim (H_7)$, to constrain and rationalize the generalized incidence rates. During the process of building the model, we not only examined the existence, non-negativity, and boundedness of the model's solution, but also defined the basic reproduction number R_0^α, as a critical metric to assess the disease's potential for spread. Building on this foundation, we derived the criteria for the LAS of the DFE P_0 and the EEP P_*, thus offering a crucial framework to comprehend the disease's dynamic progression. It is important to highlight that when $R_0^\alpha < 1$, the DFE P_0 of the model was demonstrated to be GAS. This indicates that when the spread of the disease is effectively contained, the system has the ability to self-adjust and restore itself to a disease-free state, even in the face of external disturbances or fluctuations. When $R_0^\alpha > 1$, the EEP P_* became GAS, thus indicating a persistent risk of HIV spreading within the population. Finally, our study centers on the prediction and management of the HIV epidemic in Mexico, thereby utilizing these two infection forms, $\frac{\beta_1 SE}{1+w_1S+u_1E}$ and $\frac{\beta_2 SI}{1+w_2S+u_2I}$. The analysis revealed that increasing the values of u_1, u_2, w_1, and w_2 significantly reduced the HIV-infected population and shortened the time required for the disease to be eradicated from the population.

The transmission dynamics of HIV/AIDS are undoubtedly more complex and diverse than can be adequately expressed by existing mathematical models. Thus, this study has some limitations. Potential future research directions are as follows:

- Optimal Control: Building upon the fractional-order model, we will introduce an optimal control framework to evaluate intervention strategies for the HIV epidemic. Within this framework, the condom usage rate and antiretroviral therapy (ART) coverage will be defined as time-varying control variables. A multi-objective cost-benefit function will be formulated to simultaneously minimize both the number of infected individuals and the economic costs associated with prevention and control measures. The corresponding optimality system will be derived by applying Pontryagin's Maximum Principle. Finally, the system will be numerically solved by Adam's type predictor-corrector method to compare the effectiveness of different control combinations, thus providing a quantitative basis for designing cost-effective and precise public health strategies.
- Propagation Delays: We plan to incorporate time delays into the current HIV transmission model. **Case1.** Infection Delay: This considers the time delay between an individual being exposed to the virus and becoming truly infectious. **Case2.** Treatment Delay: This accounts for the time gap between an individual's HIV diagnosis and the initiation of an effective treatment. **Case3.** Disease Progression Delay: This examines the temporal progression of HIV from the initial infection stage to more severe stages, such as late-stage HIV. We will demonstrate the existence and uniqueness of solutions for the delay model, establish the boundedness of the solutions, analyze the stability of equilibrium points, and investigate the occurrence of Hopf bifurcations. Finally, numerical simulations will be conducted to explore the dynamic behaviors of the model.

Author contributions

Mi Yang: Writing-original draft, writing-review & editing; Da-peng Gao: Supervision, writing-review & editing; Shi-qiang Feng: Writing-original draft & writing-review; Jin-dong Li: Writing-original draft & writing-review. All authors have read and approved the final version of the manuscript for publication.

Use of Generative-AI tools declaration

The authors declare they have not used Artificial Intelligence (AI) tools in the creation of this article.

Acknowledgments

This work was supported by Sichuan Science and Technology Program (2022NSFSC0558), the Fundamental Research Funds of China West Normal University (24kc003) and the Research Project on Graduate Education Reform of China West Normal University (2022XM24, 2024XM05).

Conflict of interest

The authors declare no conflict of interest.

References

1. Centers for Disease Control and Prevention. HIV and AIDS-United States, 1981-2000, *Morbidity Mortality Weekly Rep.*, **50** (2001), 430–434.
2. World Health Organization, HIV, 2022. Available from: `https://www.who.int/news-room/fact-sheets/detail/hiv-aids`.
3. G. Assembly, *Resolution adopted by the general assembly on 3 2015*, New York, United Nations, 2016. https://doi.org/10.18356/9789210026253c001
4. H. F. Huo, R. Chen, X. Y. Wang, Modelling and stability of HIV/AIDS epidemic model with treatment, *Appl. Math. Model.*, **40** (2016), 6550–6559. https://doi.org/10.1016/j.apm.2016.01.054
5. J. W. Jia, G. L. Qin, Stability analysis of HIV/AIDS epidemic model with nonlinear incidence and treatment, *Adv. Differ. Equ.*, **2017** (2017), 1–13. https://doi.org/10.1186/s13662-017-1175-5
6. S. Mangal, O. P. Misra, J. Dhar, Fractional-order deterministic epidemic model for the spread and control of HIV/AIDS with special reference to Mexico and India, *Math. Comput. Simul.*, **210** (2023), 82–102. https://doi.org/10.1016/j.matcom.2023.03.008
7. R. M. Aderson, R. M. May, *Infections diseases of humans: Dynamics and control*, Oxford: Oxford Univ. Press, 1991.
8. H. W. Hethcote, The mathematics of infections diseases, *SIAM Rev.*, **42** (2000), 599–653. https://doi.org/10.1137/S0036144500371907
9. C. Liu, J. Gao, J. Kanesan, Dynamics analysis and optimal control of delayed SEIR model in COVID-19 epidemic, *J. Inequal. Appl.*, **2024** (2024), 1–37. https://doi.org/10.1186/s13660-024-03140-2
10. C. Vargas-De-León, On the global stability of SIS, SIR and SIRS epdemic models with standard incidence, *Chaos Soliton. Fract.*, **44** (2011), 1106–1110. https://doi.org/10.1016/j.chaos.2011.09.002
11. V. Capasso, G. Serio, A generalization of the Kermack-Mckendrick determinstic epidemic model, *Math. Biosci.*, **42** (1978), 43–61. https://doi.org/10.1016/0025-5564(78)90006-8
12. L. W. Wang, X. G. Zhang, Z. J. Liu, An SEIR epidemic model with relapse and general nonlinear incidence rate with application to media impact, *Qual. Theory Dyn. Syst.*, **17** (2018), 309–329. https://doi.org/10.1007/s12346-017-0231-6
13. Q. Tang, Z. D. Teng, X. Abdurahman, A new Lyapunov function for SIRS epidemic models, *Bull. Malays. Math. Sci. Soc.*, **40** (2017), 237–258. https://doi.org/10.1007/s40840-016-0315-5
14. F. M. Al-Askar, C. Cesarano, W. W. Mohammed, The analytical solutions of stochastic-fractional drinfel'd-Sokolov-Wilson equations via (G'/G) -expansion method, *Symmetry*, **14** (2022), 2105. https://doi.org/10.3390/sym14102105

15. H. Ahmad, M. Tariq, S. K. Sahoo, New estimations of Hermite–Hadamard type integral inequalities for special functions, *Fractal Fract.*, **5** (2021), 144. https://doi.org/10.3390/fractalfract5040144

16. C. J. Sun, Y. P. Lin, S. P. Tang, Global stability for an special SEIR epidemic model with nonlinear incidence rates, *Chaos Soliton. Fract.*, **33** (2017), 290–297. https://doi.org/10.1016/j.chaos.2005.12.028

17. C. Liu, X. Yi, Z. Gong, The control parametrization technique for numerically solving fractal–fractional optimal control problems involving Caputo–Fabrizio derivatives, *J. Comput. Appl. Math.*, **472** (2026), 116814. https://doi.org/10.1016/j.cam.2025.116814

18. I. Yi, C. Liu, H. T. Cheong, A third-order numerical method for solving fractional ordinary differential equations, *AIMS Math.*, **9** (2024), 21125–21143. https://doi.org/10.3934/math.20241026

19. C. Liu, Z. Gong, C. Yu, S. Wang, Optimal control computation for nonlinear fractional time-delay systems with state inequality constraints, *J. Optim. Theory Appl.*, **191** (2021), 83–117. https://doi.org/10.1007/s10957-021-01926-8

20. Y. Luo, Y. Yuan, X. Wang, Z. Teng, Dynamic analysis of a degenerated temporal-spatial acquired immun-odeficiency syndrome model with voluntary counseling and testing awareness and antiretroviral therapy treatment, *J. Math. Phys.*, **66** (2025), 072704. https://doi.org/doi:10.1063/5.0223690

21. Y. Hao, Y. Luo, J. Huang, L. Zhang, Z. Teng, Analysis of a stochastic HIV/AIDS model with commercial heterosexual activity and Ornstein-Uhlenbeck process, *Math. Comput. Simul.*, **234** (2025), 50–72. https://doi.org/10.1016/j.matcom.2025.02.020

22. Y. Luo, J. Huang, Z. Teng, Q. Liu, Role of ART and PrEP treatments in a stochastic HIV/AIDS epidemic model, *Math. Comput. Simul.*, **221** (2024), 337–357. https://doi.org/10.1016/j.matcom.2024.03.010

23. M. Naim, F. Lahmidi, A. Namir, A. Kouidere, Dynamics of an fractional SEIR epidemic model with infectivity in latent period and general nonlinear incidence rate, *Chaos Soliton. Fract.*, **152** (2021), 111456. https://doi.org/10.1016/j.chaos.2021.111456

24. I. Podlubny, *Fractional differential equations*, Academic Press, New York, 1999.

25. Z. M. Odibat, N. T. Shawagfeh, Generalized Taylor's formula, *Appl. Math. Comput.*, **186** (2007), 286–293. https://doi.org/10.1016/j.amc.2006.07.102

26. H. L. Li, L. Zhang, C. Hu, Y. L. Jiang, Z. D. Teng, Dynamical analysis of a fractional-order predator-prey model incorporating a prey refuge, *J. Appl. Math. Comput.*, **54** (2017), 435–449. https://doi.org/10.1007/s12190-016-1017-8

27. S. G. Samko, A. A. Kilbas, O. I. Marichev, *Fractional integral and derivatives*, **1** (1993), Gordon and Breach science publishers, Yverdon, Yverdon-Les-Bains, Switzerland.

28. K. Diethelm, *The analysis of fractional differential equations, an application-oriented exposition using operators of Caputo type*, Springer, Berlin, 2004. https://doi.org/10.1006/JMAA.2000.7194

29. L. W. Wang, Z. J. Liu, X. G. Zhang, Global dynamics for an age-structed epidemic model with media impact and incomplete vaccination, *Nonlinear Anal. Real World Appl.*, **32** (2016), 136–158. https://doi.org/10.1016/j.nonrwa.2016.04.009

30. M. Naim, F. Lahmidi, A. Namir, Global stability of a fractional order SIR epidemic model with double epidemic hypothesis and nonlinear incidence rate, *Commun. Math. Biol. Neurosci.*, **2020** (2020), 38.

31. Z. M. Li, Z. D. Teng, H. Miao, Modeling and control for HIV/AIDS transmission in China based on data from 2004 to 2016, *Comput. Math. Method Med.*, **2017** (2017), 8935314. https://doi.org/10.1155/2017/8935314

32. A. Lahrouz, L. Omari, D. Kiouach, A. Belmaâti, Complete global stability for an SIRS epidemic model with generalized non-linear incidence and vaccination, *Appl. Math. Comput.*, **218** (2012), 6519–6525. https://doi.org/10.1016/j.amc.2011.12.024

33. A. Mouaouine, A. Boukhouima, K. Hattaf, N. Yousfi, A fractional order SIR epidemic model with nonlinear incidence rate, *Adv. Differ. Equ.*, **2018** (2018), 1–9. https://doi.org/10.1186/s13662-018-1613-z

34. M. R. S. Ammi, M. Tahiri, D. F. M. Torres, Global stability of a Caputo fractional SIRS model with general incidence rate, *Math. Comput. Sci.*, **15** (2020), 91–105. https://doi.org/10.1007/s11786-020-00467-z

35. A. Boukhouima, K. Hattaf, N. Yousfi, Dynamics of a fractional order HIV infection model with specific functional response and cure rate, *Int. J. Differ. Equat.*, **2017** (2017), 8372140. https://doi.org/10.1155/2017/8372140

36. P. V. D. Driessche, J. Watmough, Reproduction numbers and sub-threshold endemic equilibria for compartmental models of disease transmission, *Math. Biosci.*, **180** (2002), 29–48. https://doi.org/10.1016/s0025-5564(02)00108-6

37. A. E. Matouk, Stability conditions, hyperchans and control in a novel fractional order hyperchaotic system, *Phys. Lett. A.*, **373** (2009), 2166–2173. https://doi.org/10.1016/j.physleta.2009.04.032

38. https://ourworldindate.org/hiv-aids.